Master of Science Thesis
Lund Reports on Atomic Physics, LRAP-425
Lund University

Linus Frantzich
Sony Ericsson Mobile Communications AB
R&D Optoelectronics
Mobilvägen 10
SE-221 88
Sweden

Abstract

In this work, optical simulations as a part of product development was investigated, verified and practiced for implementation in the research and development (R&D) process of optoelectronic components at Sony Ericsson Mobile Communications (SEMC) AB, Sweden. Implementing optical simulations required several aspects such as workflow-model development and limitations to be considered and evaluated. Optical simulation software or, *ray tracers* have been commercially available for several decades and have gained importance in recent years due to higher computing capabilities and increased complexity of optoelectronic components. Following the evaluation of optical simulation software from three different software developers, software under the product name *Light Tools*® from Optical Research Associates (ORA) was selected. The procedure to successfully integrate the software for product development at SEMC included learning, verification and testing to ensure that the software had appropriate reliance for upcoming work. Products currently under development were used for verification purposes and to distinguish applications for optical simulations. Finally, simulations were carried out supporting projects in the concept phase, with the intent to learn how optical simulations could cooperate with other development processes in this project phase. In the majority of the cases, the optical simulations were successful and the outcome of the results was implemented into the projects. In those cases where the simulations did not agree with the actual result (from production), the reason was identified and noted to learn about limitations of optical simulations. In the cases of ongoing development work where optical simulations were successful, time and economical savings were considered to be significant.

Linus Frantzich

Utvärdering av optiska simuleringsverktyg vid Sony Ericsson Mobile Communications AB i Lund

Utveckling av moderna mobiltelefoner är en komplicerad process som innefattar ett långt led av spetskompetens inom vitt skilda ämnen som tillsammans syftar mot optimal konfiguration av komponenter, design, prestanda och mycket mer.

Optoelektroniska komponenter så som display, kamera, belysta knappar och kamerablixt är komplicerade komponenter som ur ett massproduktionsperspektiv kan vara svåra att integrera i mobiltelefoner. För att öka förståelsen och för att ha ett verktyg för att analysera dessa komponenter har ett optiskt simuleringsverktyg utvärderats. Mjukvaran, även kallad en *ray tracer* beräknar ljusets strålgångar enligt fysikens principer. Med hjälp av dessa beräkningar fås ett bättre utgångsläge för projekt i koncept- och utvecklingsfasen. Ökad förståelse som kan leda till färre prototypbyggen av komponenter, vilket leder till en effektivare produktutveckling.

Examensarbetet har från grunden byggt upp en process för hur optiska simuleringar implementeras i utvecklingen av mobiltelefoner. Detta inkluderar t.ex. testning, inlärning, verifiering samt utveckling av arbetsflöde för simuleringsverktyget. Eftersom produktutveckling i mycket handlar om olika komponenters samverkan behövde en gedigen kunskapsbas skapas. För detta har verktyget används i en mängd pågående projekt.

Stråloptik

I stråloptik representeras ljus av strålar. Genom att ge 3D modeller optiska egenskaper kan miljontals strålgångar beräknas för att analysera modellen. Strålgångarna kan utvärderas för att hitta potentiella problem innan detaljen blir prototyp eller massproduceras.

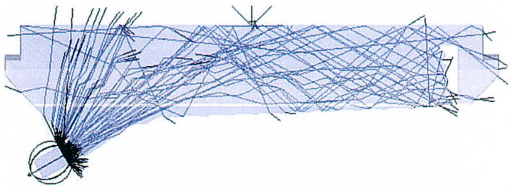

I bilderna till höger syns en ljusledare (överst) där strålgångarna från en LED (till vänster i bilden) har beräknats. I den nedre bilden visas till vänster en fotorealistisk rendering och till höger en illuminanskarta av en belyst kameraknapp. Utvärderingen avslöjar att knappen är mer belyst på vänster sida.

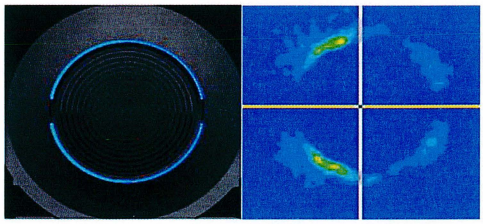

Handledare: **Allan Johansson** (Sony Ericsson) och **Johan Mauritsson** (Atomfysik, LTH)
Examensarbete 60 hp i naturvetenskap 2010
Fysiska Institutionen, Lunds universitet
Sony Ericsson Mobile Communications AB

Contents

Introduction

Sony Ericsson is a 50/50 joint venture by Sony and Ericsson established in Oct. 2001, with global corporate functions located in London and operations in all major markets [1]. Research and development is situated at several sites including Lund, Sweden. The division of optoelectronics is responsible for optoelectronic components in mobile handsets. Optoelectronic components include displays and touch sensors, cameras, camera flash sources and lenses, lit keypads, key illumination and optical sensors. With increasing importance of optoelectronic components *e.g.* larger displays and more complex illumination effects, the need for optical simulations is advancing. In many cases, optical simulations can be utilized by an optical engineer to gain knowledge on a component under development, therefore the advantages of simulations are apparent. A better starting point in *e.g.* conceptual designs can be gained for the cost of purchasing software and educating engineers to use the software. In the end, the resulting product will have better optical performance and lower development cost since fewer prototype builds lead to economical savings. Characteristic for optical component is that the behavior can be complex, such that starting designs are often difficult to improve successfully using a *trial and error* method. When the result can be seen on forehand using optical simulation, the first iterations of the improvement process can be eliminated. For these reasons optical simulations are highly motivated, and also one of the company directives to further increase for implementation in the R&D process.

Diploma work

The aim of this diploma work was to investigate current requirements for optical simulations and based on this information; choose an appropriate software simulation tool to purchase. Software capabilities requirements are important, yet practical requirements, such as CAD compatibility can also be a deciding factor. The chosen software is required to be compatible with other software already being used by *e.g.* mechanical engineers. Once simulation software that meets the specifications was found, it was tested to evaluate the software specifications. Testing was performed during a trial period of the software. Products (at SEMC) which were under development were chosen to serve for evaluation of the optical simulation software. In this way, up to date, products can be compared with simulation results. Ideally, a variety of projects should be included in this work, however, due to time limitations and other practical circumstances, two projects were selected and the aim was limited to correlation between simulation results and actual production results.

Equally important as using the optical simulations to its full potential by learning all of the aspects of the simulation software is connecting to other product development methods in the R&D process. From experience and from investigation of these other methods, this diploma work will have a detailed section covering the workflow of optical simulation which fits into the R&D process.

1 Choosing optical simulation software

Commercial optical simulation software has been available for several decades. In recent years software developers have made optical simulation software more attractive by increasing user friendliness and emphasizing on usability.

Several high-tech companies have, to smaller or larger extent, a program for optical simulations. The success in implementing optical simulations in high-tech companies has been achieved by simplifying traditionally complex software user interface to easier and better known windows-based interface. Traditionally, a team of optical engineers would be needed for performing a simulation task since the software used was complex and needed high amounts of computer resources. At present, since computer power has drastically increased and software have become more user friendly, a single optical engineer can manage a several simulation tasks at once. In cases where optical engineers are unavailable, engineers can easily learn the basics of optics and perform most analyzes and evaluation offered by the simulation software.

At the same time as optoelectronic components increase in complexity, the functionality of optical simulation software increases. In modern software, a complete package typically includes complete light source libraries of up-to-date LEDs, filament lamps, discharge lamps and natural light sources [2]. Material objects are not only defined as surface entities but can also exhibit volume effects, such as volume scattering (*e.g.* Mie scattering, Rayleigh scattering or Henyey-Greenstein scattering model). Optimization engines can find global and local target values. Later on, these functionalities will be described in greater detail.

There are several optical simulation softwares available on the market today. In Table 1 the most well known software developers and their product are presented. The level of complexity of the software in Table 1 differ between de-

Company	Product
Optical Research Associates (ORA)	Light Tools
Breault Research Organization (BRO)	ASAP / APEX
Optis	Optis Works Studio
Photon Engineering	FRED
Zemax Development Corporation	ZEMAX
Integra	Spectre

Table 1: Software developers and corresponding product name

velopers. The three most common are seen in the first three rows. Generally, they are all described by themselves to be the leading software to solve any issue related to optics that might present itself for the user. In order to actually verify the strengths and find disadvantages, the three companies were contacted for further information about the software in detail. Trial licenses were used to test each program. The main goal was to learn the basic functionalities and investigate all of the capabilities of the program. In addition the software support is an important part of the software package since it does not only include tech-

nical support but also design support from experienced engineers. Therefore, extensive testing of each software support was conducted.

To decide which software to eventually purchase, a comparison was made. It is important to remember that whichever the information might be, it is subjective to the tester (the author of this report), yet this could be the best way of comparing software since information from the software sales person is not objective. The aspects that were taken into consideration were, among others, user friendliness, cost, support, product specification and general opinion. A base for comparison was the software FRED® by Photon Engineering because of past experience from this software.

In general, ray trace software has a number of capabilities that have become more and more typical for most software packages. In the section below, some of these capabilities will be briefly described. Later on, some of these capabilities will be described in greater detail.

1.1 Ray tracing

In any optical simulation software, the main feature is the ray tracing engine which is the foundation of the software. The ray tracing engine uses rays to simulate light paths. Calculation of ray paths is based on well known physical laws, *e.g.* Snell's law (the law of refraction). Historically, ray trace engines only allowed a predefined object sequence for the rays to trace, *e.g.* through a lens system, so called sequential ray tracing. Sequential ray tracing is mainly used to simulate imaging optics. Effects such as stray light and light scattering are neglected because of its unknown object sequence. Today, most ray tracers allow non-sequential ray tracing, where no optical path is presumed. Sequential ray tracing is still available although, it is mainly preferred for imaging component analysis.

In non-sequential ray tracing, a Monte-Carlo based method [3] is used when determining the rays for the simulation. The term Monte-Carlo refers a class of computational algorithms that rely on repeated random sampling [4]. Probability cross sections are used for the ray parameters, which include *e.g.* wavelength, starting position, intensity and starting direction. The accuracy of the simulation thus depends on the number of rays traced and the desired resolution of the result. Each ray is associated with parameters from the random selection from the Monte-Carlo process and a number of calculated parameters such as surface intersections, direction alterations, energy losses and ray-splits. A receiver defines a surface of interest where the parameters of all rays on the surface are added to produce a final result such as incident power.

From the large quantity of data from a simulation, several data processing tools are available to calculate radio- and photometric intensity and illumination of a receiver surface. Filters can be set on most parameters for *e.g.* stray light analysis and finding specific ray paths. Multi CPU processing of ray traces is readily available and gives a linear increase in computational power. Ray tracing will be discussed in greater detail in chapter 2.3.

1.2 CAD compatibility

Component design is rarely performed in optical simulators. Optical simulation software is an analysis tool to analyze optical components that are designed in computer aided design (CAD) software, *e.g.* SolidWorks®. Consequently, it must be possible to import a CAD model into the software as a starting point of the simulation. Designing models using the software is possible, however, since the tools in optical simulation software are basic these capabilities are limited. There are two types of CAD import, so called *dead* objects and *living* objects. Living objects are imported CAD models with full history from the construction phase included. Changes can also be made in the design since the model is fully parameterized. Any surface of a living object is analytic such that any point of the surface can be described using an algebraic expression [5].

The CAD model in figure 1 consists of two overlapping spheres. If the two spheres comprise a living object the information stored in the model is two center coordinates (relative to a global coordinate system) and the radius of the spheres. The overlapping of the spheres is automatically included when computing the two spheres in *e.g.* a ray tracer. Dead objects can be created

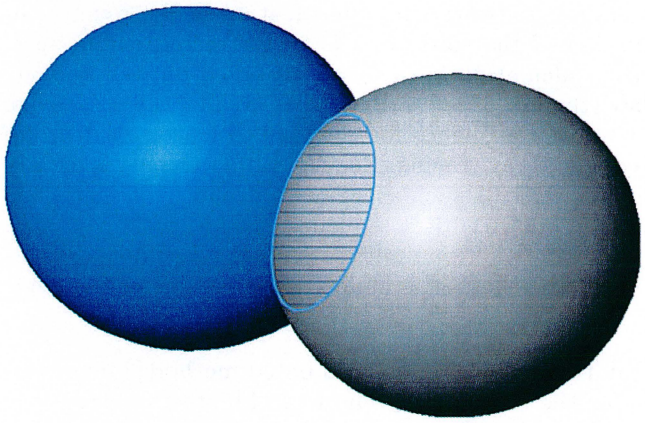

Figure 1: Two overlapping spheres

from a living object when converted into a standardized file format, such as the Standard for the Exchange of Product model data (STEP) format. If the object in figure 1 is a dead object, the information of the two spheres is lost. A matrix of points and non-uniform rational basis spline (NURBS) can describe the surfaces. When computing the object in a ray tracer, the splines are used to define the intersection point between the ray and the object. No history of how the object was created or which parts constitute an object can be seen. A living object has several advantages. Parameters such as *e.g.* length, angle, radii can be set to be optimization variables when optimizing the design. For dead objects, such values must be parameterized in a CAD program before being imported into the ray tracer.

1.3 Optimization

For parameterized CAD models, most ray trace software supports an optimization feature. Optimization parameters are defined before and are varied during the automatic optimization process. An optimization target is also defined. For a given set of values on the optimization parameters, the simulation result is compared with the target. The difference between the target and the simulation is called the merit function. The merit function is defined as a least square function and thus the optimization engine attempts to lower the merit function to zero. The mathematical definition of the merit function is decribed using the following equation [6]:

$$\text{Merit Function} = \sum W_g(\sum (W_i(V_i - T_i))^2),$$

where W_g is the weight of the merit function group g (if several merit functions are used on the same optimization parameters). W_i, V_i and T_i are the weight, current value and target of the merit function items, i, respectively. The merit function is a function of number of iterations [6].

The basic principle behind the optimization engine differs between software developers. More expensive software packages have more sophisticated optimization engines, which uses the input of the merit function and the sensitivity of the optimization values to calculate the set of optimization values in the next iteration. Algorithms to avoid local minima of the merit function can also be included in the engine [6].

In a simplified optimization method, the user defines the maximum and minimum constraints of the optimization values. The optimization engine can find incremental values between the constraints and simulate all possible combinations to create a complete merit function road map. This method is less complicated although it can be more time consuming, especially when a large numbers of optimization parameters are considered.

1.4 Photorealistic rendering

The capability to create a photorealistic rendering (PRR) based on a simulation result is available in several optical simulation softwares. In PRR, a rendering engine uses a camera view and the simulation result (calculated ray paths) to create an image of the view, as seen from an observer. To improve realism, several effects are added, such as bump-mapping, texture-mapping and shading [3]. From a design point of view, PRR can be used to comprehensively present a simulation result, as compared with the two-dimensional (2D), false color representation of a detector surface. The PRR can also be used to review design alterations and their impacts.

Typically, the PRR has variable environment parameters, *e.g.* camera FOV, background, foreground, ambient light sources and contrast settings. In such a case, standard environments can be created to compare different products in identical environments. In this way, a calibrated performance indicator is created, *e.g.* low ambient light conditions or sun light conditions.

1.5 Selecting optical simulation software

Several aspects affected the choice of software for optical simulations at SEMC. Crucial for analyzing mechanical models is the CAD compatibility. The optical simulation software must include a feature which imports CAD models. The CAD program used at SEMC does not have full compatibility with any optical simulation software. Consequently, no living CAD model imports will be possible at SEMC.

The three software packages mentioned above were tested and compared. From the comparison, Light Tools from ORA was the most suitable choice. Supplementary to the high correlation between the SEMC internal requirement on optical simulation software and Light Tools a deciding factor was conversation with colleague Greg Yow. Previously, Greg did a trial of Light Tools and worked on an RGB LED light guide with successful results. Software capabilities, such as, CAD compatibility has to be tested to find any issues that are not mentioned in the specification of optical simulation software. Greg had experience with CAD compatibility and could offer detailed information about this aspect.

1.5.1 Light Tools

After an extensive evaluation, the preferred software was Light Tools, which is developed by ORA in the United States. Light Tools have an inviting user interface with a well structured system of features. The learning curve of basic features in Light Tools is steep, learning simple simulations is straight forward and can be learnt in a matter of days. Less clear is the ray treatment which is "built in", which means that some properties are not seemingly disclosed. Of course, experimenting in Light Tools with ray treatment is possible and very useful. All of the capabilities described in the previous sections are supported by Light Tools, in some cases also in further extent than described.

The flexibility of the Windows-based user interface has some limitations, *e.g.* limited history of set parameters. Although lists of parameters can be generated, script based simulations have a larger overview of the simulation setup. In Light Tools, macros can be written using C++ or MatLab®to supply commands to Light Tools and automatically post-process simulation data.

The cost for purchasing Light Tools varies as different capabilities are purchased individually. A powerful computer is preferred (in this case, double quad core Intel Xeon®processors with 16GB of physical memory) to simultaneously handle several simulations, CAD programs and programming interfaces. For distributed simulation, *i.e.* when distributing the calculation to the available CPUs, the time savings are typically linear with the number of CPUs [7].

2 Theory

In this theory section, topics of relevance for this diploma work are briefly dealt with. In order to understand how to specify *e.g.* materials and light sources in a ray tracer, knowledge about the physical processes is important. Equally important is to have a general feeling about parameter sensitivity since all optical simulations are to more or less extent approximations of the theory. Most of the optoelectronic components used in modern mobile handset devices will be described, including basic principles, applications and specifications of the component. In addition, sections will be devoted to ray tracing and light matter interaction, which discusses how optical simulations are performed and ray treatment in *e.g.* scattering events, respectively.

2.1 Optoelectronic components

2.1.1 Light emitting diode

In mobile devices, Light Emitting Diodes (LEDs) are the primary light sources due to their low power consumption, high luminous flux, low heat dissipation and small geometrical size. LEDs are the only light source used in mobile devices for the exception of Xenon discharge lamps (in camera flash applications). The LED industry is highly developed and increasingly advanced LED light sources are continuously introduced. Typical applications for LEDs in mobile devices are: RGB LEDs for multicolored indicators, white LEDs for display backlight, high output LEDs for camera flash, extra-compact LEDs for keypad and button illumination. Infrared (IR) LEDs are used for proximity sensors.

Basic principle of the LED

Light emitting diodes incorporate a group of light sources fabricated from semiconductor materials. In semiconductor materials, the electron conduction band is empty and the electron valance band is full. The forbidden energy gap between the conduction band and the valance band, called the band gap, is small in a semiconductor, see figure 2. When the band gap is large, the material is an insulator and when the bands are overlapping the material is a metal. The band structure is used to explain several macroscopic properties of materials, such as electric conductivity and thermal conductivity.

In semiconductors, electrons in the valance band can be thermally excited to the conduction band and consequently, light is emitted by the semiconductor material when electrons are recombining with holes across the band gap. The photon energy is equivalent to the band gap energy. In steady state, no photons are produced in the semiconductor material, although if a voltage is applied, light is produced from the injection of charge carriers which recombines in the material. The described phenomenon is called electroluminescence [8]. If the semiconductor material is *doped* a dopant material is blended into the semiconductor and spread randomly in the crystalline structure of the host semiconductor mate-

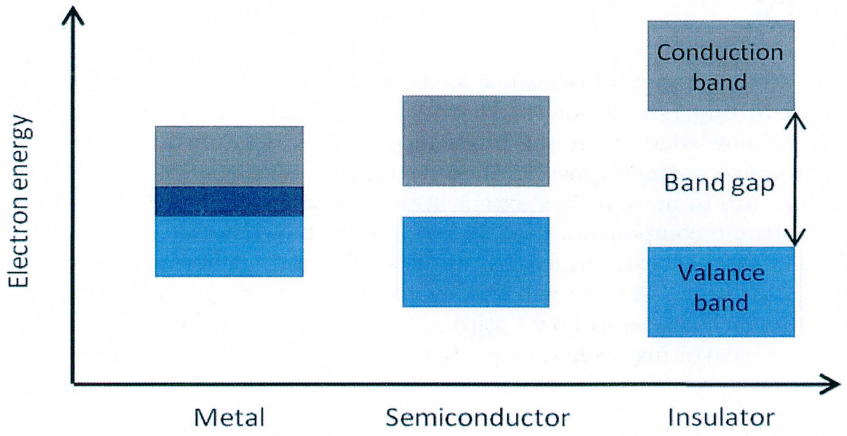

Figure 2: Band gap structure of a metal, semiconductor and insulator, respectively

rial. Dopant material contains either one more electron (n-dopant) or one less electron (p-dopant) than the host material. The result is discrete energy levels placed inside the band gap, in proximity to the continuous bands, see figure 3. The discreet energy levels are called *donor level* and *acceptor level*. Their

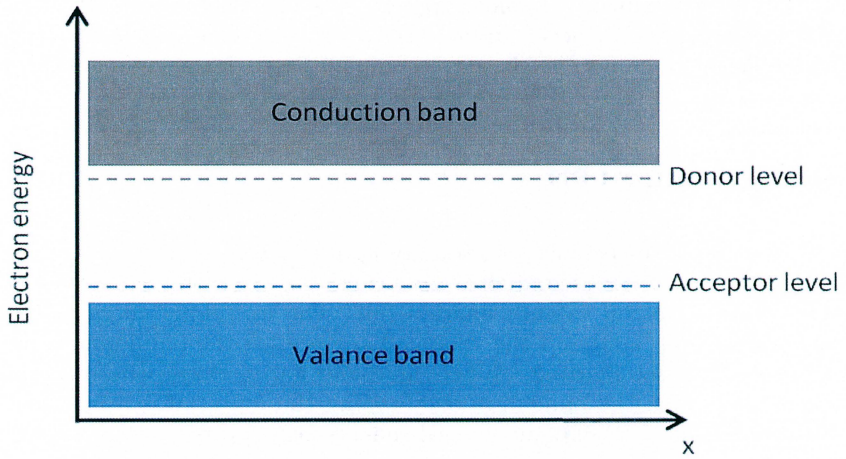

Figure 3: Dopant materials can be added to the semiconductor. The energy levels of the dopants are discrete energy levels in proximity to the continuous bands

placement can be explained by the dopant atomic core which differs with one elementary charge unit from the host material. Thus, the coulomb potential differs slightly for the valance electrons and holes of the dopant atoms. The valance electrons of the dopant material can thermally excite to the conduction band since thermal energy needed is very small, see figure 3. In summary, when the semiconductor material is for example, n-doped, additional electrons are

placed in the conduction band. In figure 3, the material is both p and n-doped. However, materials can also be either p-doped or n-doped. Interesting properties are found when combining one p-doped and one n-doped semiconductor.

When combining a p-doped and one n-doped semiconductor in metallurgical contact, a *pn-junction* is formed. As the two semiconductors are in contact, a sequence of actions occurs [8]:

1. The high concentration of electrons in the n-doped part and holes in the p-doped part diffuse over to the opposite side of the pn-junction. The diffusing charge carriers recombine on the other side resulting in localized, positively charged ionized donor atoms on the n-region and negatively charged ionized acceptor atoms on the p-region.
2. As the amount of localized ionized donor and acceptor atoms build up, a built-in electric field is created in the pn-junction, see figure 4, which starts preventing the diffusion of charge carriers between the two sides.
3. In time, an equilibrium conditions is met, when the diffusion rate of holes and electrons is equal to the drift currents associated with the built-in field, see figure 4. In this way, no net current flows across the junction. The pn-junction has formed a region of localized ionized atoms which forms a capacitor. The region is called the depletion region.

The built in voltage of the pn-junction prevents the large amounts of electrons on the n-doped side from recombining with the large amounts of holes on the p-doped side. By biasing the pn-junction with an external voltage in the forward direction, and thus eliminating the built in voltage, the high amount of injected charge carriers from the external source can freely recombine with injected holes in the valance band. When charge carriers recombine, a photon is created to conserve energy. The basic model described above is valid for early generation LEDs, today LEDs can be exceedingly advanced.

In solid-state physics, electrons are described as quantum mechanical *electron waves* (wave-particle dualism) in the periodic crystal lattice of the semiconductor material. The band gap of forbidden energies of the electrons can be explained with energies of the electron satisfying Bragg's law of diffraction and thus canceling the electron wave function. The wave function of the electron in the periodic crystal lattice can be described using Bloch wave solutions [9]:

$$\varphi_{n\mathbf{k}}(\mathbf{r}) = e^{i\mathbf{k}\cdot\mathbf{r}} u_{n\mathbf{k}}(\mathbf{r})$$

Where $\varphi_{n\mathbf{k}}(\mathbf{r})$ is the wave function as a function of spatial coordinates as $r = (x, y, z)$, $e^{i\mathbf{k}\cdot\mathbf{r}}$ is a plane wave in free space and $u_{n\mathbf{k}}(\mathbf{r})$ is a periodic function in space that has the same periodicity as the lattice coulomb potential. The wavevector, $\mathbf{k}$, is related to the momentum vector (direction) of the electrons in the crystal.

For period lattices, the energy of the electron is heavily dependent on the direction of motion since the period structure with direction in space. Therefore, it is conventional to plot the electron energy as a function of electron wavevector,

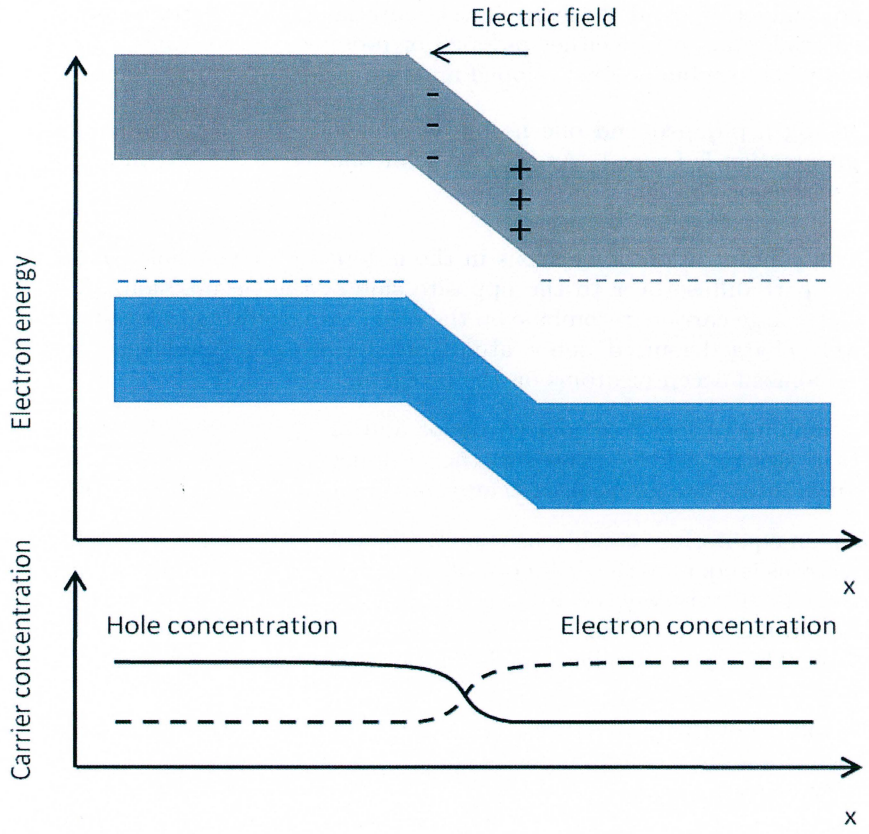

Figure 4: In equilibrium, the pn-junction forms a build-in voltage band structure

also called an $E(\mathbf{k})$ diagram. Electrons in the conduction band accumulate with the wavevector giving the lowest possible energy and holes in the valance band accumulate with the wavevector giving the highest possible energy. If these two wavevectors are identical, the semiconductor is said to have a direct band gap, see left hand side of figure 5. If the wavevectors differs, the semiconductor is said to have an indirect band gap, see right hand side of figure 5. For photonic devices, a direct band gap is essential since photons carries very small amounts of momentum compared with the electron momentum. Thus, for a radiative deexcitation in an indirect band gap structure, several photons are needed in a multi-photon interaction (to conserve momentum). Since multi-photon interactions are very rare, non-radiative deexcitation will most prominently occur. Consequently, indirect band gap materials such as Silicon are highly unsuitable for photonic devices.

In summary, the LED is a forward-biased pn-junction, which relies on spontaneous emission of photons when injected charge carriers (electrons and holes) recombine in the direct band gap semiconductor material. LEDs are highly effective as large amounts of the injected charge carriers recombine in radiative processes. Spontaneous emission of photons has no coherent properties and

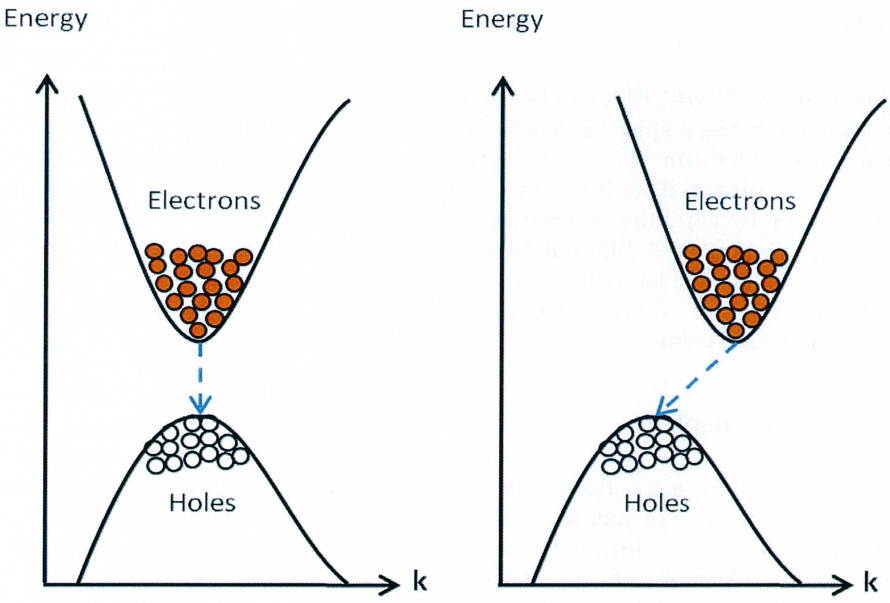

Figure 5: Direct (left) and indirect (right) band gap structure

photons are emitted in all directions from the active layer. Typically, the LED is encapsulated in a plastic coating, formed as a lens to increase the optical performance by directing the light in the preferable direction, serve as index-matcher to reduce Fresnel losses and increasing the critical angle to avoid total internal reflection (TIR). In 1962, Gallium-Arsenide (GaAs) was the first LED to be fabricated [10]. Today, advanced photonic devices can be created, giving rise to an entirely new field of photonics called band gap engineering, which is the field of altering the band gap of photonic semiconductor materials to new properties. LEDs exist from ultraviolet (UV) to IR wavelengths.

White LED

Since optical action in semiconductor materials occurs between energy levels the spectral bandwidth is limited to solid state broadening effects of the transition between the energy levels. In general, the spectral bandwidth of LEDs is 10-30 nm, as opposed to gas transition where the bandwidth is very narrow. In order to produce white light, a high energy transition LED (blue) can convert some of the output photons in a series of stokes shifts to produce the components needed for white light. A fluorescent material, similar to the powder in fluorescent lamps, is used for this purpose. The semiconductor material is typically Indium-Gallium-Nitride (InGaN) which has a band gap which produces the blue photons.Alternatively, white light can be produced by combining one red, one green and one blue LED, also called an RGB LED.

RGB LED

As mentioned above, RGB LEDs can be used to produce white light. Fundamentally, the human eye has a spectral sensitivity function, the luminosity function, which peaks around 550 nm. Thus, to create white light (equal amounts of RGB components when observed with the eye), RGB LEDs can produce white light or any other color by carefully combining the RGB components. As the RGB LEDs are comprised of three different LEDs, they are not spatially overlapping. A diffuser is normally used to reduce the spatial dependence of the output color, also called color mixing. When color mixing is successful, the output light is observed as one single color.

2.1.2 Flat panel display

Flat panel display (FPD) is a collective name, comprising any display technology which is flat, in contrast to former generation cathode ray tube (CRT) monitors. Flat panel displays have revolutionized numerous fields of consumer electronics, most prominently TV monitors and have also enabled mobile handsets with displays. Several technologies are available to produce FPDs, and can be owed to the advancements in semiconductor technology. The most common FPDs can be seen in Table 2. In the mobile handset industry, LED backlit LCDs are the

FPD Technology
Plasma display panel (PDP)
Liquid crystal display (LCD)
Oraganic light-emitting diode (OLED)

Table 2: Common flat panel display technologies

most common FPD technology. However, in recent years, other technologies are emerging. One of these is active-matrix OLED (AMOLED) display. For more information on OLED technology, see reference [11].

The image on a display is described using a matrix of points. Each point contains three numbers. The three numbers represent the red, green and blue (RGB) values of the point also called the *RGB components*. When displaying the image, depending on the technology, different ways of translating the RGB components into light exist. Displays use a matrix of *pixels*, each containing three *subpixels*, representing the RGB components, see figure 6. Digitalization requires the RGB components to be described using 256 integer numbers per component (for 16.7 million colors displays). When the contents of the image file is altered the subpixels need to be able to alter state. One way of achieving a display is by using a liquid crystal. In the the following section the LCD will be described in greater detail.

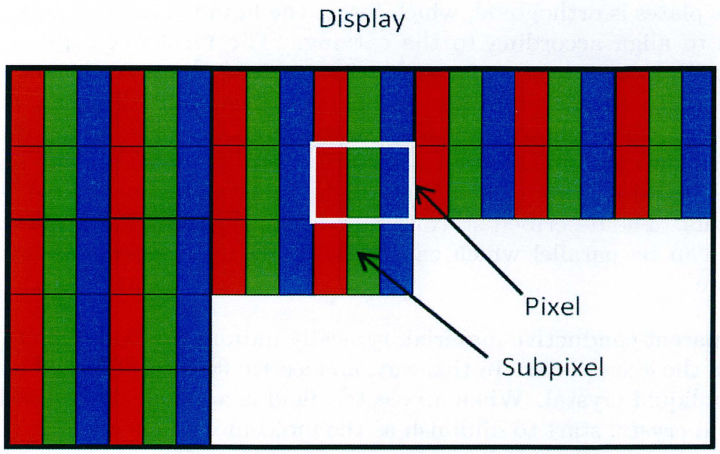

Figure 6: RGB subpixels constituting a pixel in a display

Basic principle of the LCD

To alter the state of the subpixels in an LCD a liquid crystal is placed between glass plates. Two global crossed polarizers are placed in front and behind the glass plates. A global white light source, behind the bottom polarizer is used to illuminate the liquid crystal. Using a local electric field over the liquid crystal each subpixel can be locally affected such that it alters the polarization of the light when traveling between the crossed polarizes. Thus, 256 discrete voltages (for 16.7 million colors displays) are used to create a set of 256 different light transmission values through the cell. Finally before displaying the image, a color filter is placed on each subpixel, corresponding to the component color (red, green or blue). The component color is transmitted through the filter and the renaming wavelengths are absorbed.

To change the polarization state of light traveling through the cell, a liquid crystal with birefringent properties is used. Birefringent materials are structured materials such as crystals which exhibit different index of refraction depending on the axis of orientation of the crystal much like electrons in semiconductor crystals. The phenomena of birefringence causes the two component polarization states transverse electric (TE) and transverse magnetic (TM) to exhibit different index of refraction. Consequently, the light components travels at different speeds, allowing the total polarization state (which is the resultant of the TE and TM components) to change. In certain liquid crystals the molecules are anisotropic and not randomly orientated. In some LCDs the liquid crystal molecule itself is positive uniaxial, meaning that it has two axis of symmetry resulting in birefringent properties [8].

Carving in the two glass plates is used to create a preferred direction of orientation for the liquid crystal adjacent to the glass plates. Several configurations of polarizers and liquid crystals exist, however, the most commonly described in literature is the twisted nematic (TN). In TN field effect displays, the carving

of the two glass plates is orthogonal, which forces the liquid crystal in proximity to glass plates to align according to the carving. The mechanical properties of the liquid crystal cause it to twist gradually between the glass plates. The twisted liquid structure with birefringent properties, if carefully designed, act as a phase modulator which allows light that is polarized from the first polarizer to be modulated into the polarization state accepted by the second polarizer. Thus, when the liquid is in its passive state, light is allowed to pass though the crossed polarizers. The described state is called referred to as *normally white*. The polarizers can be parallel which causes the LCD to be *normally black* in the passive state.

A grid of transparent conductive material, typically indium tin oxide (ITO), can be deposited on the glass plates. In this way, an electric field can be established, locally, over the liquid crystal. When an electric field is applied, the twisted nature of the liquid crystal start to diminish as the molecules starts aligning to the electric field. As the electric field "untwists" the liquid crystal, the phase modulation properties are affected such that the modulated polarization state at the second polarizer is not allowed to fully pass. The component of the modulated polarization in the direction of the second polarizer is allowed to pass which reduced the luminous flux of the light accordingly. Thus, when the voltage over the liquid crystal is strong, the liquid if fully untwisted and no light is allowed to pass the second polarizer. Voltages between 0 and the fully closed (or fully open) voltage can be used to control the light output. The ITO grid defines the subpixels.

The microprocessor of the LCD addresses the ITO grid to display an image. There are several ways of addressing the grid of pixels. In non-complex LCD design used in *e.g.* alarm clocks direct addressing can be used, see figure 7. Each pixel then has a separate routing. For larger displays, *e.g.* in mobile handsets with 854x480 pixels (WVGA format), direct addressing is impossible since the large number of data lines would be hard to implement. To address larger grids

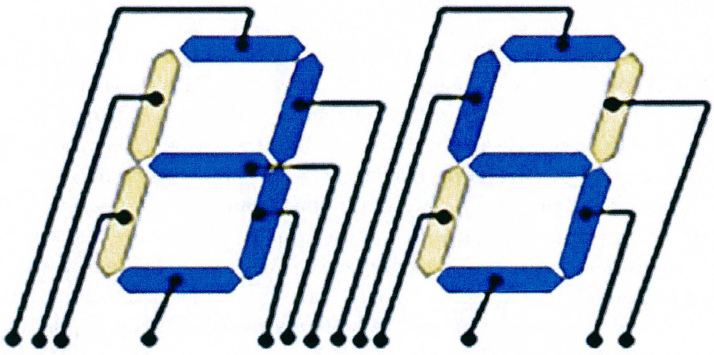

Figure 7: Direct addressing commonly used to address the pixels in a non-complex LCD design

of pixels, active multiplex (AM) addressing is commonly used, see figure 8. A column driver connects each column of pixels serially and a row driver connects

all rows in of pixels serially. Thus, to activate a pixel, the corresponding column and row driver is activated. To connect the drive voltage to ground level, a field effect transistor (FET) located in the pixel is connected to both the row and column driver. The gate allows two pixels to simultaneously activate even when sharing the same row or column driver by storing the voltage. The stored voltage in the FET is used to activate the pixel when the row or column driver is busy activating other pixels. In this way, by scanning the rows vertically, an image can continuously be displayed. A matrix of FETs are applied to a thin film, also called thin film transistor (TFT)[12]. To improve the luminous flux

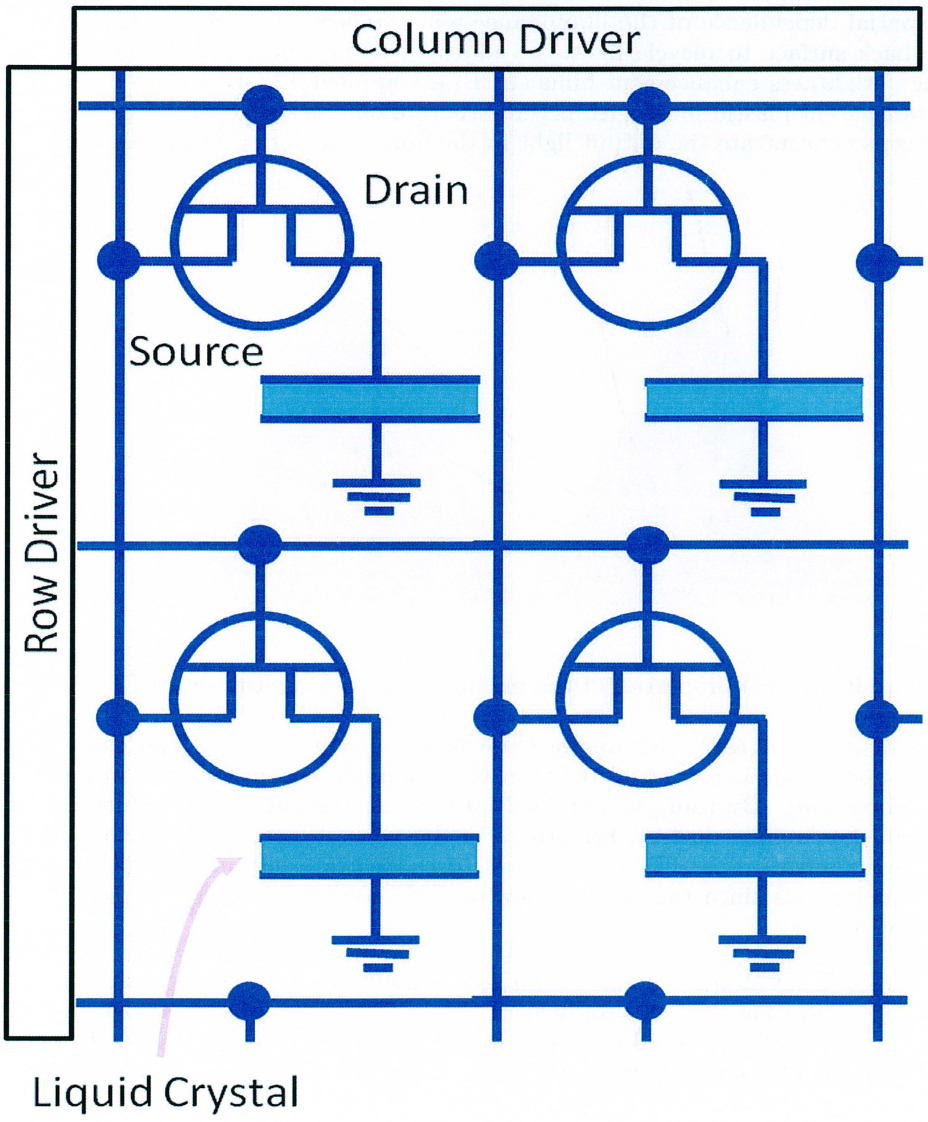

Figure 8: Electrical scheme of four elements in an active multiplex addressing circuit

in sunlight conditions, the sunlight source itself can be utilized by applying a reflective coating on parts of the first glass surface. Consequently, sunlight can be reflected on the coating and filtered in the color filter. A disadvantage of a reflective coating is the reduced low ambient light performance. A LCD with this design is called a transreflective LCD.

In mobile handset displays, the white backlight is typically produced by phosphorous LEDs due to their compact size. For larger devices a cold cathode fluorescent light (CCFL) source is traditionally employed, although, in recent years, LED backlights have become readily available. Diffusers are used to eliminate spatial dependence of the illuminance and a reflective sheet can applied to the back surface to recycle light. In addition, to further increase the illuminance brightness enhancement films (BEF) are applied [13]. BEFs are based on a transparent plastic sheet with prism structure on one surface, see figure 9. The prisms concentrate the output light in the normal direction of the display,

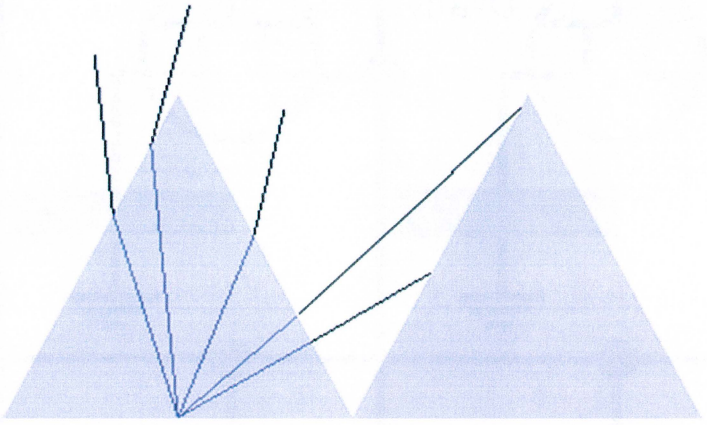

Figure 9: Optical properties of the prism structure constituting a BEF

as seen in figure 9 (rays with angles close to normal incidence). The choice of prism apex angle is a tradeoff between viewing angle and brightness (in the normal direction). By using two crossed BEF films, the effect can be further increased. For mobile devices, brightness in the normal direction is preferred over viewing angle. The BEF can be used to concentrate output light off the perpendicular axis since the normal viewing direction of a mobile handset is somewhat off axis.

There are both advantages and disadvantages of the LCD [12]. One of the main advantages is the low cost of producing LCDs. The entire LCD is two large polarizer sheets and the liquid crystal is injected between to glass plates. The structure of the ITO conductor and the color filters determines the shape of the pixel.

One of the main disadvantages of the LCD is light efficiency. The global backlight has a constant luminous flux, thus, when reducing the flux using the liquid

crystal and the crossed polarizers, light is removed. Additionally, the color filters spectrally remove most of the white light to select a certain color. The global backlight is the main disadvantage when comparing to LED array displays, where each pixel is a light emitter itself, which lowers the power consumption linearly when reducing the luminous flux of the pixels. The contrast ratio is also affected by the constant backlight since some light always escapes the crossed polarizers when operating in OFF-state. In LED array displays the contrast is theoretically infinitely high due to nonexistent backlight. In reality, the contrast in LED array displays is not infinitely high due to reflections in the display.

In figure 10, a typical stack up of an LCD display can be seen [14]. Note the thickness of the entire LCD (not including the protective glass) is no more than 1.4 mm. When implemented into a mobile handset, a touch sensor can be included between the LCD and the protective glass.

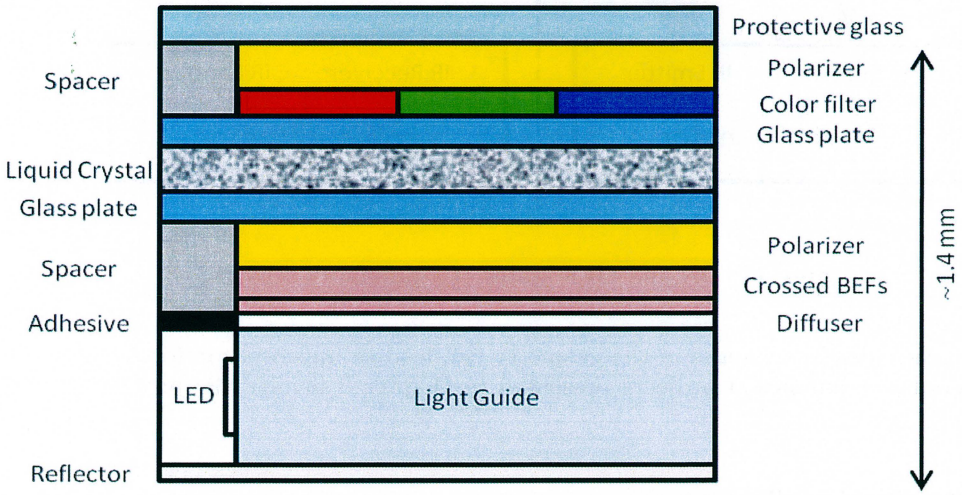

Figure 10: Stack up of an LCD display

2.1.3 Proximity sensor

In mobile handsets, several sensors monitor the environment. One of the sensors is the proximity sensor which monitors the presence of an object in proximity of the handset. The idea is to detect when the handset is in proximity to the users ear or cheek so that the touch sensor is disabled. The touch sensor is disabled to avoid accidental activation during phone calls. The proximity sensor consists of two components, a LED and a photodetector, both operating in the IR region. The basic principle is to detect reflected IR radiation which has scattered on an object in proximity. When no object is in proximity no IR radiation is detected, see figure 11. Proximity sensors can be sensitive to optical short circuit, *i.e.* when the IR radiation, by internal reflection, is transmitted from the IR emitter to the IR receiver without exiting the mobile handset. Optical simulations can be performed to evaluate short circuit issues. From the

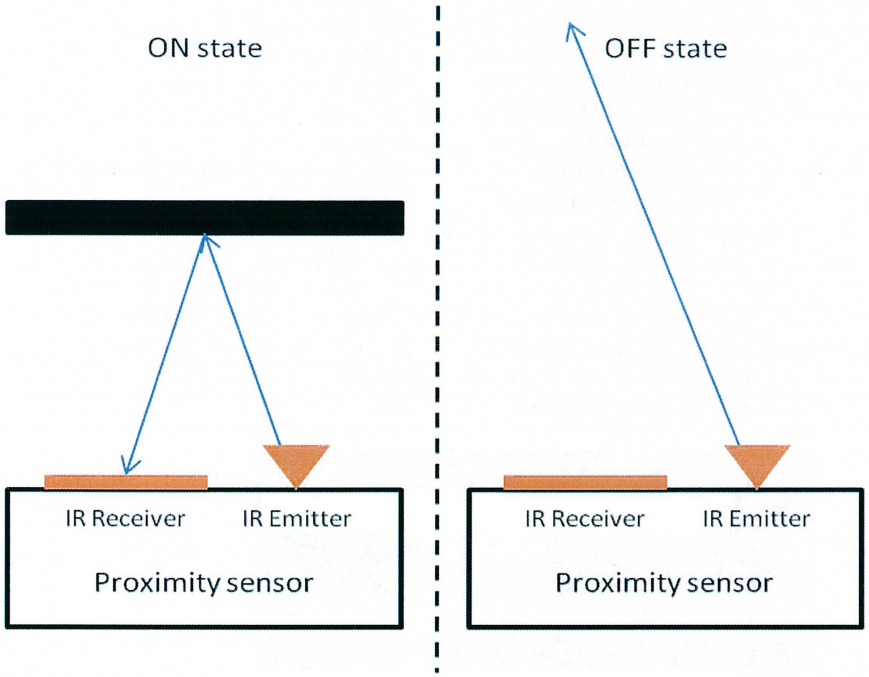

Figure 11: ON and OFF states of a proximity sensor

simulation results, changes in the geometry can lead to improved performance. Some of the simulation projects presented in chapter 3 involve the proximity sensor.

2.1.4 Ambient light sensor

Displays are dependent on the ambient light level for optimal functionality, *e.g.* lowering the backlight current in low light conditions to improve power consumption. The ambient light sensor (ALS) is a photodetector with a spectral sensitivity similar to the human eye and has a wide dynamic range of several orders of magnitude in illuminance [15].

The ALS must be designed to avoid detecting direct light from the backlight LEDs in the display, which can be problematic in low light conditions. A window is used, much like the window in the proximity device, to hide the sensor. Light with certain incident angles on the sensor risk not reaching the ALS when placed far away from the window. From an evaluation of the geometry, some certain angles can be investigated using a point source with low divergence angle. To improve angular sensitivity, a diffusive surface can be placed on the surface of the window closest to the ALS. To test the performance of the ALS in an optical simulation, a hemispherical source can be placed over the ALS window. In this way, all possible entrance angles of the light can be evaluated at once.

2.1.5 Camera

The human eye is an extremely sophisticated tool for presenting the world around us in a comprehensible way. The camera device is the mechanical equivalence of the human eye and thus one of the most advanced components in mobile handsets. The camera device can be divided into three main parts: Optics, image sensor and image signal processor (ISP). The optics of the camera

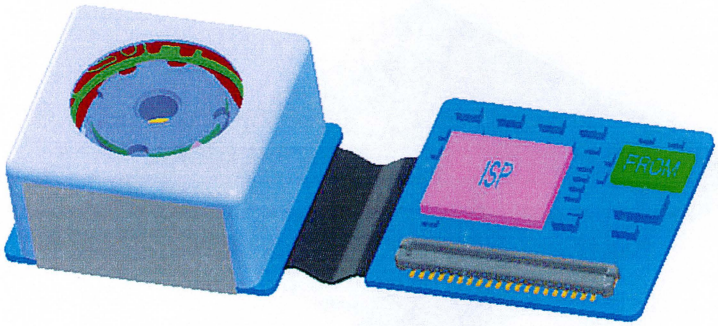

Figure 12: 3D model of a camera used in a mobile handset

consists of a lens package, typically one glass aspheric lens and three plastic lenses to correct for Seidel aberrations. For more information on optical aberrations, see reference [16]. All lenses are anti-reflection (AR) coated to minimized Fresnel reflection at the refractive index boundary (lens surface). AR coating increases light collection efficiency and minimizes stray light in the camera. In order to create sharp images of objects at different distances from the camera, the lens-to-sensor distance must be variable (consider the lens formula). The lens to sensor distance is normally controlled using voice coil motor (VCM) technology [17]. The VCM is an actuator which counteracts the spring-loaded lens package. The linearity of the spring force equation creates a linear direct current-vs.-lens position relationship. The resolution of the VCM is typically 180 positions over a few tenths of a millimeters stroke. Elaborate algorithms compare different images (from different lens positions) to find the best focus of the scene. This function is called auto focus (AF) and is readily available in handset device cameras. Besides the lens package and the VCM, the optical components include a reflective type IR-filter since the image sensor is sensitive to IR radiation [18].

The image sensor is based on semiconductor technology and functions much like an inverse LED. Instead of generating photons by injecting charge carriers, photons incident on the detector elements (pixels) creates a current, called the photocurrent. To increase light collection efficiency, microlenses can be applied to each detector element. When photons are incident on a detector element, electron-hole pairs are created either by band to band transitions or forbidden band gap energy level (from impurities or dopants) transitions [10]. The created charge carriers increase the conductivity of the detector element which has two metallic contacts. Integrated electronics are used to read out the photocurrent from each pixel element. A current gain mechanism is used to amplify the small

photocurrent.

To create color digital images, each detector element is associated with a color filter. The color filter array is arranged to represent the spectral sensitivity of retina in the human eye. Thus, green pixels comprise 50 % of the pixels, the red and blue components comprise 25 % of the pixels each in a *Bayer* filter, see figure 13. Unlike a global shutter, where an entire image is captured at once,

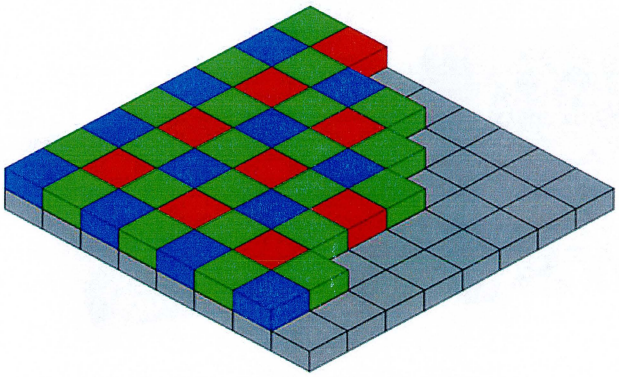

Figure 13: Schematic figure of a bayer filter placed over the photodetector array [19]

some solid state photosensors use a technique called rolling shutter. The basic principle of rolling shutter is seen in figure 14. Since only one row can be read

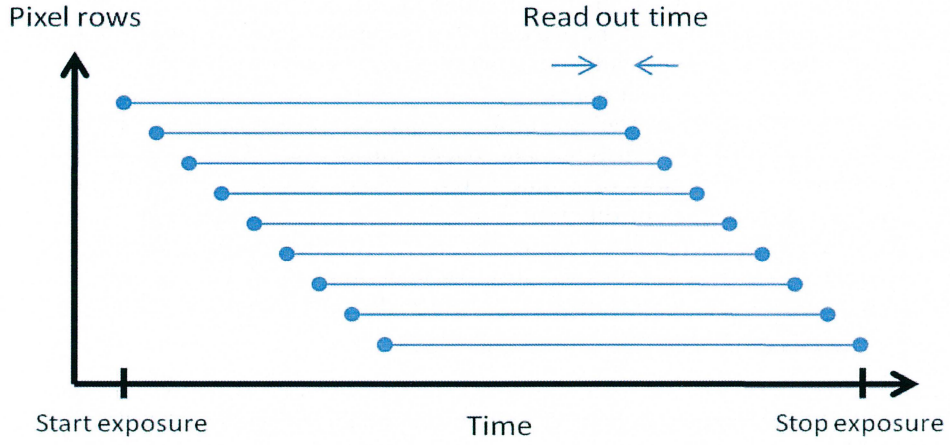

Figure 14: Rolling shutter read out scheme

out at once, rows are sequentially delayed with the read of time to ensure rows are read out, one at a time. In this way, the resulting image is not representing a discreet time. Rolling shutter artifacts are normally unnoticeable; however, artifacts can have significant impact, especially when capturing high speed events.

Currently, a typical image sensor comprise 3-5 Megapixels (MP) in low and mid-end handsets. In high-end handsets up to 12 MP is readily available. In high-end handsets a second camera can be included, often a chat camera for video calls which has lower performance (VGA resolution, *i.e.* 0.3 MP) when compared to the main camera. The chat camera is typically smaller than the main camera and does not include AF or high imaging quality.

2.1.6 Camera flash

When capturing images in low ambient light conditions, image quality can be improved by including an external light source in the mobile handset. Two types of light sources for camera flash applications exist, the Xenon discharge flash and the white LED flash. In this report the white LED flash will be described. For information on Xenon discharge flash see reference [20].

High luminous flux LED of phosphorus layer type, explained on page 16, is commonly used for camera flash applications in SEMC handsets. The luminous flux of the LED is a function of the supplied current. In products, the driving current is up to 1.5 A. At this current a luminous flux of 300 lm is achievable. Using a camera flash lens, parts of the output light can be directed inside the camera FOV. With a luminous flux of 300 lm and a well designed Fresnel lens, an illuminance of 210 lx is readily available at 1 m distance, which is comparable to normal indoor lightning. In low ambient light environments the exposure time of the camera is normally longer to collect more light. If the camera has a rolling shutter, the LED must illuminate the entire start-to-stop time (see figure 14), typically 250-350 ms.

One of the main problems with increasingly strong semiconductor light sources is the high level of heat dissipation from the high driving currents involved [21]. When driving a LED at 1.5 A the temperature increases heavily with time. For 250-350 ms duty cycles, the LED will almost reach the maximum allowed temperature if proper heat sinks are used. Insufficient heat sinks will cause the LED chip to become overheated. At high temperatures, the optical properties are affected, the efficiency decreases leading to lower luminous flux. The spectrum also becomes shifted towards the blue, such that the white light becomes purplish. At extreme temperatures, the LED chip can melt and become permanently disabled. The anode and cathode connectors are often used as heat sinks by extending their surface area. Nearby metal components such as metal screws and shield cans can also be used as heat sinks.

2.2 Optical components

In mobile handsets, some types optical components are reoccurring, *e.g.* camera flash lens. In this section these components will be described for a more comprehensive understanding when, later on, discussing the simulation projects. This section is focused on general properties, *e.g.* fabrication or material for mass production of the optical components and related tradeoffs.

2.2.1 Fresnel / TIR lens

Historically, Fresnel lenses have been used for several centuries in non-imaging applications, most prominently in naval context, such as light house lenses and light beacons [22]. The main feature of the Fresnel lens is the eliminated bulk material of a lens which lowers material costs, lowers weight and decreases the size of the lens, as seen in figure 15. The bulk can be eliminated since the optical action (refraction) only occurs at the surface of the lens. The Fresnel surface curvature is identical to the conventional lens surface and thus has the same optical properties. In mobile handsets and other compact devices the decreased size of the Fresnel lens when comparing with conventional lenses is an advantage. The Fresnel lens is not optimal for imaging, as such, typical usage is camera flash applications. The Fresnel lenses are excellent at focusing

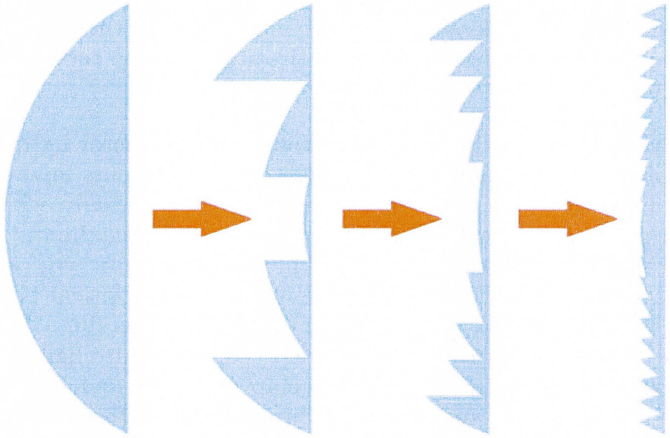

Figure 15: Explanatory figure of the Fresnel lens geometry [23]

collimated beams, however considering the geometry, highly divergent beams are shadowed by the Fresnel grooves. In camera flash applications, the divergent beam from the flash LED is not fully compatible with a Fresnel lens. The outer grooves can be replaced with TIR elements which reflects the light towards the scene, see figure 16. The most common material for the Fresnel lens is optical grade polymethyl methacrylate (PMMA), which is a thermoplastic material suitable for injection molding. Injection molding is a production process where thermoplastic granulates is melted and injected with high pressure into a mold cavity (sometimes called a tool) to create a plastic object of almost arbitrary

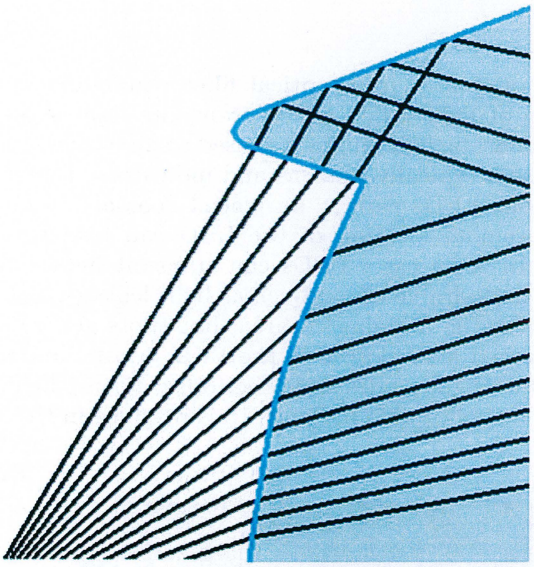

Figure 16: Ray trace of the outer TIR elements of a Fresnel lens

shape [24]. For injection molded Fresnel lenses a limiting factor is the tip radius of the Fresnel valleys and peaks, see figure 17. A tip radius of zero is ideal since a perfect corner can be created. For injection molding a tip radius around 0.05 mm is normally achieved. The surface area which is subject to the tip radius geometry does not direct light from the LED correctly and thus, a larger tip radius than zero, lowers the optical performance.

For camera flash applications the Fresnel lens forms the LED output beam to

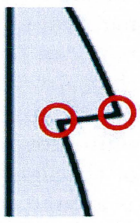

Figure 17: The red circles marks the Fresnel valleys and peaks

illuminate a scene. A tradeoff between flash efficiency and corner illumination falloff has to be considered. The flash efficiency is the amount of output light from the lens that falls within the camera field of view (FOV) compared to the total output light. The corner illumination falloff is the illuminance at the corner of the FOV compared to the center illuminance. When focusing the light, the Fresnel lens flash efficiency increases and corner illumination falloff increases. The parameter lens gain (LG) is also of a performance indicator. The lens gain is the ratio between the illuminance in the center with and without the lens. For a typical flash LED and PMMA Fresnel lens the LG is 2 - 3.

2.2.2 Light guides

The term *light guide* originates from optical fiber communication where the optical fiber is a type of light guide which transmits light signals over long distances. In mobile handsets, light guides are used to direct light from a LED to an area to be illuminated, typically buttons and indicators. Due to mechanical and electrical limitations LEDs cannot be placed coaxially with the area to be illuminated. The remote location of the LED can lead to stray light if not properly guided. In some cases LEDs can transmit light through plastic materials, resulting in undesirable effects such as light leakage. When LEDs are not placed coaxially with the illuminated area, hot spots generally appears in the part of the illuminated area closest to the LED. Most illumination effects needs extensive work with light guides and other optical components to create a homogeneous effect. The light guide in figure 18 is produce in the same process

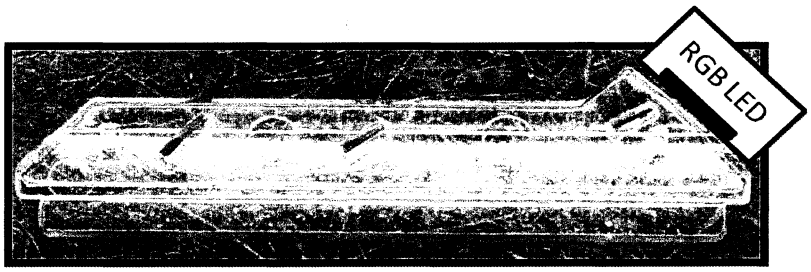

Figure 18: Example of light guide including an RGB LED

are PMMA Fresnel lenses. The most common material used is optical grade PMMA. The example light guide in figure 18 is used to couple a single side firing (SF) RGB LED into the short side (right). The aim was to illuminate the entire lower side. For light guides of the type above, hot spots are the main problem. To eliminate hot spots, geometrical cuts are introduced in the plastic part. Additionally, the entire plastic part can be blended with certain particles to create a diffusive appearance of the part which increases the illuminance homogeneity. In flat light guides for *e.g.* keypads or QWERTY keyboards hot spots are typically minimized using white dot patterns, see figure 19. Dots of white ink are placed on the bottom of the light guide. The size of white dots varies, although, in general their size is around 180 μm in diameter. When light traveling inside the light guide is incident on the white dot, light is scattered in all direction (lambertian scattering). In some of these directions, light goes back to internal reflection inside the light guide. In the other case light is refracted in the top surfaces, see figure 19. The density of white dots controls the luminous flux at that area. In optical simulation softwares, the placement of white dots (or other light outcoupling mechanisms) can be calculated to achieve a homogenous light output using one or several LEDs.

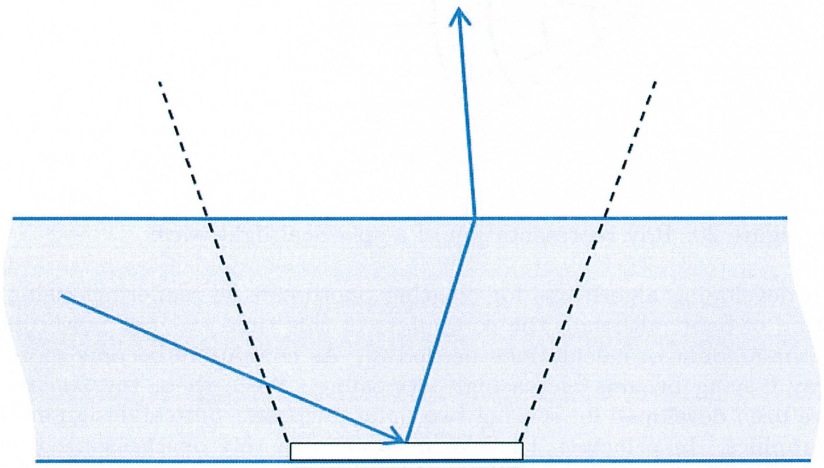

Figure 19: Example of light guide including an RGB LED

2.3 Ray tracing

For several decades, geometrical ray tracing has been employed for analysis of optical systems. [25]. In computational ray tracing light is represented by rays with a direction normal to the wavefront of a light wave, see figure 20. This simplification is normally referred to as geometrical optics. In the 1960s, scien-

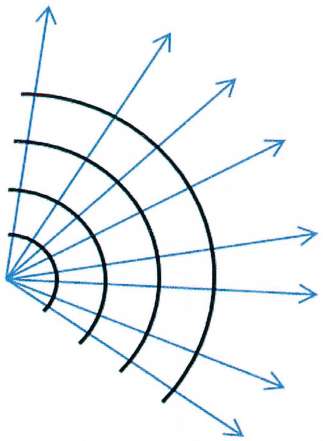

Figure 20: Ray representation of a spherical light wave

tists started developing algorithms for creating photorealistic renderings using the simulation of light, although the computers of this time was not powerful enough for the amount of calculations needed [3]. As computers became more powerful, ray tracing became increasingly appealing. Since then, ray tracing engines have been developed for serving two main purposes: optical design and computer graphics. In principle, the two purposes can rely on the same ray tracing engine. In the field of computer graphics the aim is a realistic image. In optical design, the aim is simulating the actual optical events. This difference allows computer graphic ray tracers to be simplified in order to gain calculation performance. At present, real-time ray tracers for computer graphics is readily available.

Although the ray tracing algorithms in computer graphics and optical design are much alike, there are some differences between the fields. The main difference is the tracing direction. In computer graphics the aim is creating a 2D image of a digital 3D scene. In other words, which of the photons from the light source are incident on the 2D image? To answer this question, the ray tracing engine in computer graphics calculates ray paths with origins in the 2D image, so called *backwards ray tracing*. In this way, the number of calculations can be heavily reduced since it can be presumed that rays will form an image in the 2D image plane. In optical design, there is no presumption regarding the ray paths. Where the rays will end up is dependent on the design. Backwards ray tracing is available in most optical simulation softwares and can be used in special cases when information concerning ray direction is available. In optical design, the

ray information is more detailed to contain information such as polarization and phase.

Common for any ray tracing engine is the definition of a ray. The two main components of the ray are the ray origin and the ray direction [3]:

$$R_{\text{origin}} = R_0 = [X_0\ Y_0\ Z_0],$$
$$R_{\text{direction}} = R_d = [X_d\ Y_d\ Z_d],$$

where R_d is normalized, *i.e.*

$$X_d^2 + Y_d^2 + Z_d^2 = 1$$

In some ray tracers, R_d is normalized to the power of the ray. Object surfaces are typically coincident with ray origins to define a light source. For living objects, *e.g.* a spherical light source, the sphere is defined using the following formalism:

$$\begin{aligned} S_c = [X_c\ Y_c\ Z_c] &\qquad \text{Sphere's center} \\ S_r &\qquad \text{Sphere's radius} \\ [X_s\ Y_s\ Z_s] &\qquad \text{Sphere's surface,} \end{aligned}$$

where the surface points (defined with high resolution and accuracy) are given by:

$$(X_s - X_c)^2 + (Y_s - Y_c)^2 + (Z_s - Z_c)^2 = S_r^2$$

In figure 21, a 2D representation of the formalism above is seen; note that the vectors are not light rays even if the origin, direction and radius are all vectors. The light ray is defined using the main components stated above as (see blue line in figure 21):

$$R(t) = R_0 + R_d \cdot t$$

where $t > 0$ (the ray is only defined in the direction of the ray direction vector). The Monte-Carlo simulation method randomly selects starting positions for each ray within the user-defined limits (the sphere surface points in this case). The second main component, direction, is also randomly selected. At this stage,

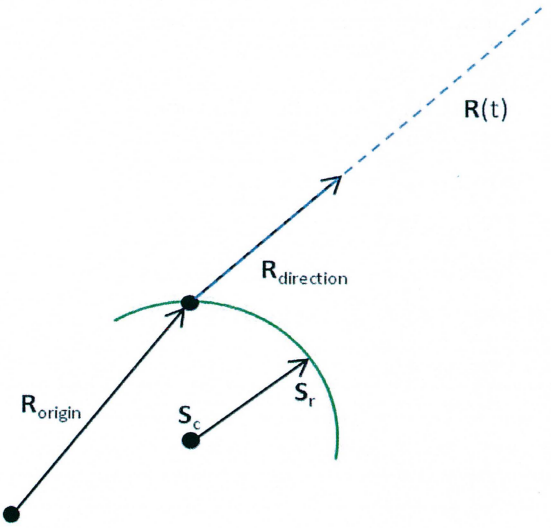

Figure 21: Ray with an origin at the surface of a sphere shown i two dimensions

filters can be applied to limit the Monte-Carlo selection, *e.g.* emittance angle by evaluating the ray direction vector.

If the sphere defined above is an object intersected by a ray created from a light source (figure 22), the ray coordinates, $R(t)$ are compared with the coordinates of the sphere surface. For the sphere object, such a comparison would yield two solutions (both sides of the sphere, as marked with red circles in figure 22). The closest intersection is found by comparing the distance from the intersection to $R(0)$ for both intersections. For detailed information on these calculations, see reference [3]. In the simulation data, each intersection stores a number of ray parameters, such as, traveled distance and incident direction. The object (the sphere in this example) parameters decide the interaction with the ray. If transparent, the refractive index is used to calculate the angular deflection due to refraction and Fresnel losses (if enabled) using Snell's law and the Fresnel equation. A detector surface is needed to collect information. It is common to collect additional information in a simulation, for example, stray light or far field analysis using several detector surfaces. Much like an image sensor, the detector surface has detector elements or pixels which collect rays. A tradeoff between image resolution and computational time is needed. If many pixels are used, high resolution results can be simulated. However, if many pixels are used many rays are needed in each pixel to have a good signal-to-noise ratio (SNR). The Monte-Carlo method introduces noise since ray parameters are randomly selected. At the detector surface the rays are computed pixel-by-pixel. If the detector is photometric (identical spectral response as the human eye) each ray power is weighted, depending on the wavelength, to the luminosity function and cumulatively added together. The computed luminous flux at each pixel and the pixel size are used to calculate an illuminance (in lx) map for the detector. Other detectors are available, such as luminous or radiant intensity (lumen per steradians or watts per steradians, respectively) and RGB raster

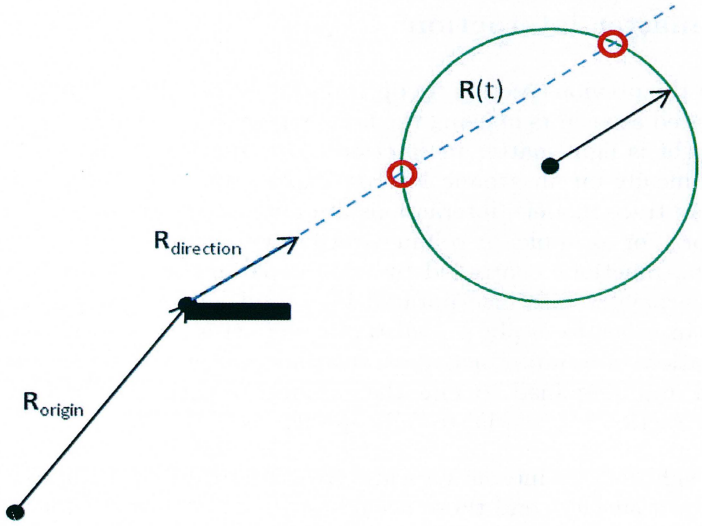

Figure 22: A ray with two intersection points on a sphere (red circles), shown in two dimensions

charts (displaying the photometric RGB components in each pixel).

In many optical simulation softwares, phase can be included to simulate wave optics phenomena such as interference. The optical path length (*i.e.* including the decreasing in velocity when traveling in high refractive index medium) is used to find the phase at the detector. The phases of all rays are superimposed to find the resulting phase.

2.4 Light-matter interaction

As explained in the previous section, in optical simulations, light is represented by rays and treated as vectors obeying the laws of geometrical optics. The main interaction of light is light-matter interaction. The interaction can be treated quantum-mechanically on an atomic level to explain the physical phenomena occurring. In ray trace models, interactions are applied as a response function to the ray vector. For example, in volume scattering, complex interactions give rise to scattering functions controlled by several parameters. In ray tracers, most of these parameters are incorporated in a total angular scattering cross section. Thus, in order to apply a realistic angular cross section to a model, theoretical equations are unproductive. Consequently, measurements are typically employed and simplified to find the response function. Knowledge on light-matter interaction is essential to fully specify the model.

In ray tracers, light-matter interactions are divided into two categories: those occurring on object surfaces and those occurring in the volume occupied by an object. In some cases they can be used to describe the same physical property, although with different degrees of simplification. In other cases they can both be applied to the same object simultaneously.

Computationally, volume scattering calculations are more demanding for two reasons. Events occur during the entire optical path through an object which readily increases the number of computations performed. Additionally, volume scattering calculations often lead to rays irrelevant for the simulation output, *e.g.* rays absorbed by the object due to long scattering path inside the object. In the equivalent situation using surface scattering, absorbed rays are handled at the surface. Thus, absorbed rays are incorporated in the surface property. The interaction mechanisms explained below are specific for Light Tools, although, the formalism could be valid for other optical simulation softwares as well.

2.4.1 Volume interaction

Volume interaction is mainly concentrated to volume scattering events, however, additional volume interactions exist, such as volume absorption. Volume scattering is much like a random walk with a defined mean free path before changing direction, see figure 23. The angular scattering cross section can be either user-defined or calculated (using input parameters in scattering models). The scattering events continue until either the ray power is below the ray threshold or it exits the material. The simplest scattering model is Rayleigh scattering, which describes the interaction between photons and very small particles (on the order of the wavelength of the light). The angular cross section of scattered particles follows a $I(\theta) = cos^2(\theta)$ relationship. The electric field in the light wave causes the charged atoms in the particle to oscillate with the same frequency, which in turn emit light of the same frequency [26].

The Mie scattering model is valid for particles where the particle size is larger than the wavelength of the light. The large size causes the electric field to be spatially dependant over the particle which induces a more complicated angular

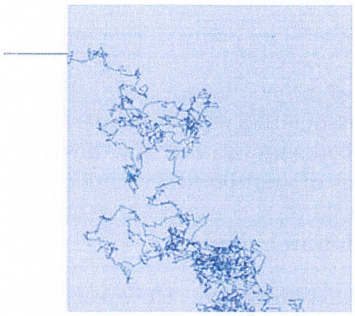

Figure 23: A ray entering (from the left side) an object with volume scattering properties

scattering cross section. The angular scattering cross section for Mie scattering can be calculated using input parameters such as particle size and index of refraction of particles [27].

Empirical models for volume scattering exist and are frequently used in biomedical optics. One of these models is the Henyey-Greenstein approximation which uses a mathematical expression to determine the angular cross section. The Henyey-Greenstein formula can be written [28]:

$$p(\theta) = \frac{1}{4\pi} \cdot \frac{1 - g^2}{(1 + g^2 - 2g \cdot cos(\theta))^{3/2}},$$

where p is the probability of scattering in θ direction (zenith angle). The constant g can take values from -1 to 1. When $g = 0$, the angular scattering cross section is equal in all directions of space. When decreasing g, a backwards scattering lobe is formed at the expense of the forwards lobe. In the limiting case when $g = -1$, the probability for backscattering is unity. Similarly, when $g = 1$ light can only scatter in the forward direction. The $\frac{1}{4\pi}$ component is a normalization factor to enforce the integral over 4π steradians is unity [29]:

$$\int_0^{2\pi} \int_0^{\pi} p(\theta) sin(\theta) \, \mathrm{d}\theta \, \mathrm{d}\phi = 1,$$

where ϕ is the azimuth angle. In biomedical optics, most volume scattering materials have been characterized using the Henyey-Greenstein approximation and several other constants to accurately model light propagation in *e.g.* human blood vessels. The simplicity and flexibility of the formalism can be used to create first approximation models for light scattering in other mediums. The angular scattering cross section can be estimated based on the visual impression of the sample which is modeled.

2.4.2 Surface interaction

Surface interactions are defined at object boundaries. Each object consists of several surfaces, each surface is associated with a property. A multitude of surface properties is available in optical simulations, *e.g.* mirror, absorber, grating, Fresnel lens property, several types of angular scattering cross sections, etc. The Fresnel lens property is an example of a complex refracting geometry which is incorporated as a response function in a surface.

Most surface properties are self-explanatory. However, scattering events are worth a more detailed discussion. Two types of scattering properties exist, simple scattering and advanced scattering. Simple scattering comprise Lambertian, Gaussian and CosNth scattering. Light which scatters on a lambertian surface has equal illuminance on a surface surrounding it. For example, if a point on a surface is a lambertian emitter and a hemisphere is placed centrally over the point, the hemisphere will be equally illuminated over the entire hemisphere surface. Mathematically the intensity of the point source is defined as:

$$I(\theta) = I_0 \, cos(\theta),$$

where I is the scattered intensity with angle θ and I_0 is the incident intensity. At normal incidence, the intensity will be I_0 multiplied with a constant which depends on the solid angle of the viewer at normal incidence. At an angle, θ, the intensity is lowered by factor of $cos(\theta)$. However, the solid angle which covers the same area has to be increased with a factor $cos(\theta)$, which will give the same intensity as the normal observer [30].

Rays affected by the lambertian surface can be either reflected, transmitted or both. If both are applied, rays can either be probabilistically scattered into either direction or split into two rays. For stray light analysis, split rays are preferred. When a lambertian surface is used as a diffuser, it can be useful to discard the rays which are not directed towards the detector to save calculation time. If a low amount of rays hits the lambertian surface, the ray can split up in several rays to improve the accuracy of the result.

As mentioned, a diffuser can be modeled as a lambertian surface. If the diffuser is of reflective type, 70 % reflectance can be assumed. For transmissive diffusers the transmittance has to be defined and is heavily dependent on the thickness of the diffuser. The high reflectance of diffusers is due to an inherent property of volume scattering. Light which scatters in a volume is most probable to exit through the entering surface if the mean free path is much smaller than the sample thickness. If a diffuser is modeled with volume scattering, this effect is incorporated in the volume scattering property.

In fact, lambertian surface scattering can replace volume scattering for non-complex geometry by adding an optical density to the object. Optical density is defined as:

$$D = \log_{10}(\frac{1}{T}),$$

where T is the transmittance per unit of length. In other words, optical density is a function which exponentially increases the loss of power of the rays when propagating inside an object. This is the analogy to light traveling in a scattering medium. For example, consider a medium with 25 % transmittance. When placing two mediums of this kind in optical contact, the transmittance after the second medium is 25 % of the 25 % transmitted light from the first medium, *i.e.* $0.25 \cdot 0.25 = 0.0625 = 6.25\,\%$.

When replacing volume scattering with surface scattering computational time can be lowered up to several orders of magnitude. Visually, this can be understood by considering figure 24. The large amounts of directional changes

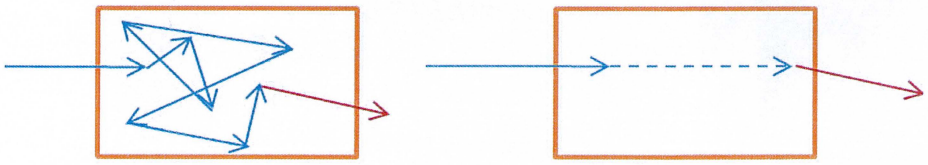

Figure 24: Simplification of volume scattering by using one surface scattering surface

inside the object are non-relevant. Moreover, many of the rays exit through the entering surface, in which all the calculations are non-relevant. A disadvantage is that rays in the surface scattering method have only one directional change which can lead to non-correlation for complex geometry. Theoretically, this could be solved by introducing planes of lambertian scattering with 100 % transmission inside the object.

In experiments (in the optical simulation software), replacing volume scattering with surface scattering has been successful, even for semi-complex geometry, see figure 26. Although the correlation is not 100 %, computational time could be reduced by a factor of 100. The semi-complex object in figure 25 has several complex shapes and varying thickness. Not all surfaces are lambertian. In many cases, the surface is specular or semi-specular. The definition of complete specular, which is the direct opposite of diffuse, is a mirror. The ray has undergone no change in direction from the optical axis of the ray. Semi-specular reflection is also called Gaussian scattering because the angular scattering cross section is described using a Gaussian function [30]:

$$I(\theta) = I_0 \exp(-\frac{1}{2})(\frac{\theta}{\sigma})^2,$$

where I is the scattered intensity with angle θ and I_0 is the incident intensity. The width of the function is given by σ. In figure 27, a 2D representation of

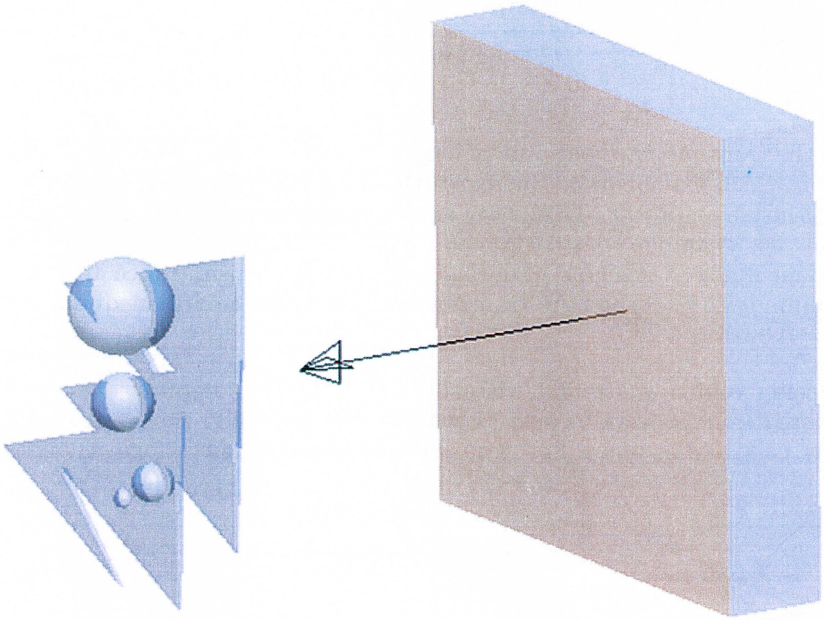

Figure 25: A surface emitter (orange surface) emits a collimated beam in the direction of the arrow on a receiver placed on the other side of the semi-complex object

the Gaussian function is seen. The amount of specularity can be controlled to match a certain surface. Typically, the full width at half max (FWHM) is used to characterize the width. A semi-specular surface has a FWHM of 20 degrees. It is important to notice that the angle θ is the deflection from the angle the ray had before the scattering event, as opposed to lambertian scattering where the incident angle is irrelevant.

Another way of characterizing surface scattering is using the CosNth model, where the angular scattering cross section can be expressed [30]:

$$I(\theta) = I_0 \, cos^N(\theta),$$

where $N = 0, 1, ..., \infty$. The mechanism can be understood by considering the limiting cases when $N = 0$, $N = 1$ and $\lim_{x \to \infty}$. When $N = 0$ there is an equal probability that the ray is deflected in any direction, as $I(\theta) = I_0$. When $N = 1$ the formalism is equal to lambertian scattering, with the difference that in the NthCos model, the incident angle influences the deflection. Consequently, when the incident angle is 0 (normal of the surface) the two scattering models are identical. However, when the incident angle becomes larger, there is a larger difference. The difference is explained in figure 28. Finally, when N goes towards infinity, specular reflection is employed.

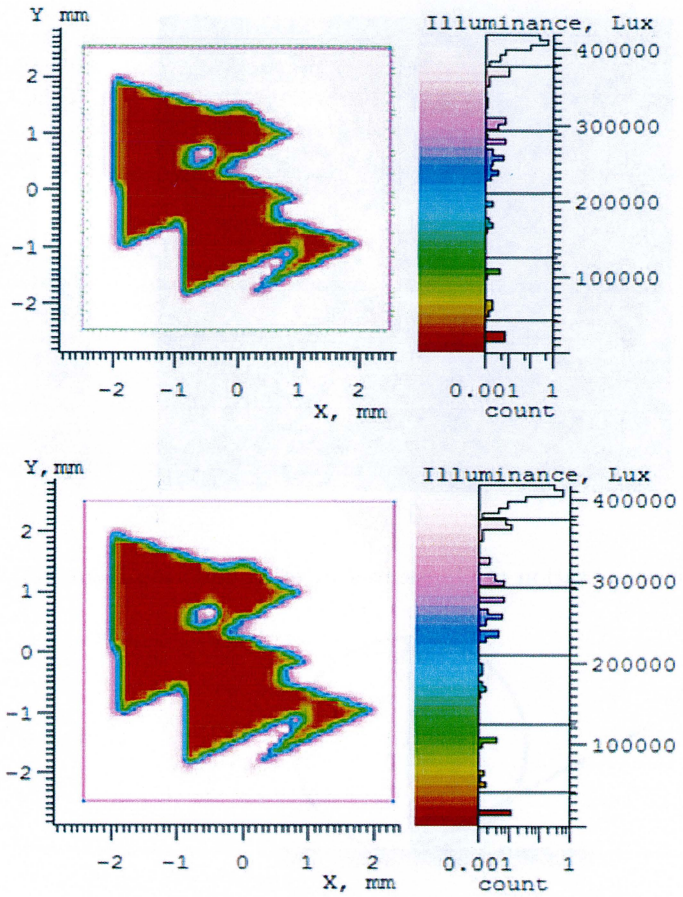

Figure 26: Results from the simulation prepared in figure 25. Top: Surface scattering (lambertian, 100 % transmission and optical density = 4.13. Bottom: volume scattering only, uniform angular scattering cross section

When a more precise characteristic is needed for a material, bi-directional reflectance/transmission distribution function [31] (BRDF/BTDF respectively) can be measured. The BRDF is a complete reflectance characteristic, *i.e.*, light is incident in all zenith and azimuth angles in the northern hemisphere. For each angle, the entire reflectance distribution is measured using a gonioreflectometer. The gonioreflectometer has two arms that can move independently in a hemisphere. On one arm a calibrated light source is situated. On the other arm a calibrated photodetector is placed. BTDF is measured in an identical way except the detector is placed in the southern hemisphere. The resulting measurement is four dimensional (two spatial surface coordinates and two angles (incident and reflected). Optionally, wavelength can be the fifth dimension. Many optical simulation softwares support BRDF/BTDF data. The appropriate angular scattering cross section distribution is found by analyzing the incident angle of the ray and finding the reflectance angle and power in the BRDF data.

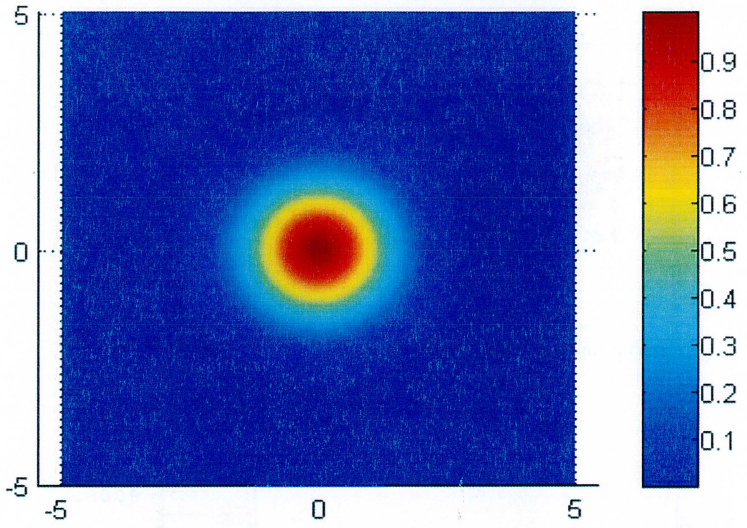

Figure 27: 2D representation of Gaussian scattering function (semi-specular)

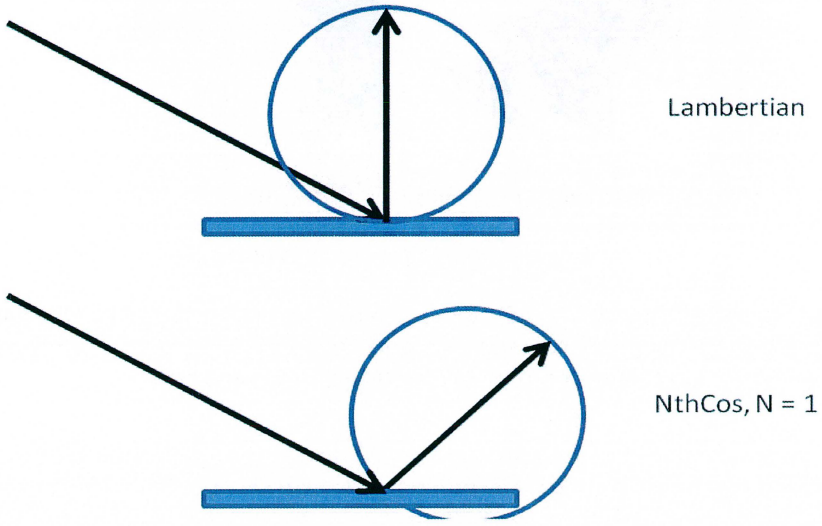

Figure 28: The difference between lambertian scattering (top) and NthCos scattering, $N = 1$

3 Simulation projects

The main assignment of the diploma work was evaluating Light Tools on ongoing projects, preferably in the concept phase. Although, in reality most simulations were performed on projects in the development phase. Concept phase projects are most suitable for optical simulations since results can be used in two important ways:

- Finding issues before development phase (building prototypes)
- Suggested changes have a realistic probability of influencing the prototype design

A total of five months (of ten) was spent working on the simulation projects to gain a full understanding of the software capabilities, CAD compatibility, workflow development, third-party interaction, simulation-production correlation and tradeoffs, optical design, mechanical design and more. The experience of working with the simulation projects is needed to fully evaluate the abilities and limitations of optical simulations. Not specifically explained in the simulation project work are issues that were unexpected when initiating the simulations. These issues could only be detected when working with the software.

The results and conclusions of the simulation projects were carefully documented to create a flexible database of information that could be accessed when needed to. In the sections below, the highlights of the simulation results is seen. In some projects the project definition can change after simulations have assisted in solving an issue or evaluated a design. In those situations, simulation results are presented although the solution were never implemented in the prototype build.

For each project, discussions on the simulations are included. However, a more general discussion for the simulation project work is found under the chapter Conclusion & Future. Any photographic images were taken with a Nikon D700 digital camera. Since any unreleased products are confidential, emphasis on discretion is employed. For this reason, the project name has been changed.

In general, each simulation follows a specific workflow model. In Appendix A, a workflow model for several simulation tasks is described in greater detail. The workflow model consists of step-by-step instructions and comments for setting up an optical simulation.

Project overview

Six projects were covered during the diploma work. Project 1-4 are projects in concept- and development phase. Project 5-6 were used for learning purposes. The simulation aim, result and suggested solution for each project can be seen in the items below:

- Project 1
  - → Camera flash
    - → The aim of the simulation was investigating the camera flash solution and evaluating the performance. An agreement between simulated beam profile (as seen from camera FOV) and a captured photograph of the camera flash could be established.
  - → Proximity sensor
    - → An issue concerning the proximity sensor was observed during the development phase. The issue was related to the white plastic cover causing optical short circuit in the proximity device. The issue was identified and a solution was suggested. The solution was verified in a prototype build.
- Project 2
  - → Camera flash
    - → Two lenses were suggested by the third party supplier both with advantages and disadvantages. In the simulation performed, one of the lenses had unappealing inhomogeneity. The simulation suggested one of the lenses over the other and the concept project could make the choice based on the results. The chosen lens was verified with measurements to correlate to the simulated performance.
  - → Chat camera stray light analysis
    - → The chat camera protective glass had an unusual geometry. The geometry could induce stray light in the chat camera. To test the affect on stray light, two simulations were performed. One simulation when including the protective glass and one simulation when it was removed. The difference between the simulation result showed only statistical noise from the Monte-Carlo selection process.
  - → Main camera stray light analysis
    - → Much like the chat camera stray light analysis, a chrome ring around the main camera protective glass could possibly induce stray light. The chrome ring induced a high level of stray light. However, in production the geometry of the chrome ring changed due to production limitation. The new geometry favored directing rays away from the main camera. In prototypes no unusual amounts of stray light could be detected.
  - → Keypad backlight
    - → The light guide used to illuminate the keypad in this project was removed. To illuminate the keys the silicone support mat of the keys was extended towards the LEDs to act as a light guide. The simulations suggested that the illumination effect would be acceptable. In prototypes, using the silicone mat as light guide was successful.

- Project 3
  - → Proximity sensor
    - → In the concept phase of this project, the proximity sensor and ambient light sensor was benchmarked against a operational reference project (which used the same components) by assigning identical properties making the geometry the differentiating factor. The simulation results suggested a lower performance in Project 3 compared with the reference project in terms of optical short circuit. The results could be used to explain for mechanical engineers, the importance of improvement of the proximity sensor in the concept phase. An improve geometry was introduced and new simulations suggested no optical short circuit issues.
  - → Ambient light sensor
    - → The ambient light sensor window had substantial geometrical issues which was revealed in simulations. A few minor design alterations improved the performance several orders of magnitude. The issues were not intuitive at first approach, however, they became clear when observing the simulation.
- Project 4
  - → LED status indicator
    - → A design of a LED status indicator was first attempted by a trial-and-error process. Optical simulations could be used to eliminate several iteration stages in this process. The resulting illumination profile could be visualized using photorealistic rendering capabilities of the simulation software and displayed for product planners. In prototypes the illumination profile was highly correlated to the photorealistic rendering.
- Project 5
  - → Camera flash
    - → In this simulation a tolerance investigation of the LED to lens distance was performed to increase the knowledge of mass production related effects. Investigations indicated that the lens was acceptable to some tolerances despite a small focal length.
- Project 6
  - → QWERTY keyboard
    - → The complex structure of the QWERTY keyboard in this project was most likely close to the limitations of what the simulation software can handle. Further approximations is needed to successfully optimize the white dot pattern of the keyboard. Further investigation is needed to ensure that further approximations can be implemented.

3.1 Project 1

3.1.1 Camera flash

In project 1, the outer casing of the handset device is non-planar at the location of the camera flash. To maintain the handset profile, the camera flash lens required a non-planar outer surface. Optically, non-perpendicular surfaces deflect the light from the flash LED in an off-axis direction. Methods exist to create an off-axis output beam using an alteration in the lens [32]. However, since the curvature magnitude was limited, no compensating effects were implemented. A section view of the camera flash lens in project 1 can be seen in figure 29. The lens is a refractive-TIR hybrid comprising two TIR rings and a refractive surface in the center. The bulk material is used to fill the space from the LED to the surface of the mobile handset. The consequence of a curved outer surface

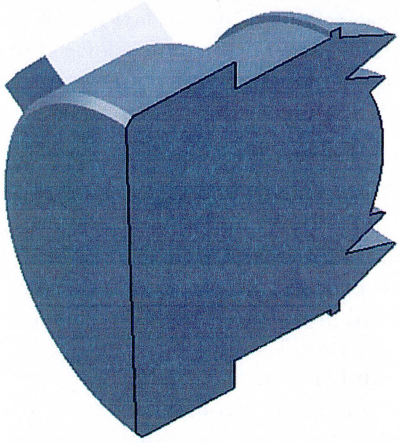

Figure 29: Cross section view of the camera flash lens in Project 1

is a tilted output beam which can miss camera scene. This effect already exists since the camera and camera flash are biaxial. However, the biaxial placement of the camera and camera flash is minimal and the negative effects associated do not increase with distance to the scene since the two axes are parallel. To evaluate the potential issue with the tilted output beam, an RGB Monte-Carlo simulation was performed for 1 meter distance between flash LED and scene.

To display the simulation results in a comprehensible way, RGB raster charts can be used. Since no other light sources are included in the simulation the parts of the scene where the flash LED does not illuminate are black. This gives the impression of how the camera flash profile would appear in a dark room.

In figure 30 (left), the final result of the simulation is seen. The RGB simulation can be compared with the photographic image taken with the camera device which as seen in figure 30 (right). The detector area represents the FOV of the camera at 1 meter distance. The simulation suggests some uniformity is-

sues, with visibly lower illuminance on the left side of the scene. The simulation also suggests lower illuminance in the center of the scene. When comparing the

Figure 30: RGB Raster chart (left) of the beam profile and photographic image (right) of the beam profile in Project 1

simulation with an actual photograph with the handset camera, the uniformity issue can be confirmed. However, the photographic image is overexposed in the center, which makes it impossible to determine the correlation on the lowered center illumination issue. Small differences in illuminance is difficult to capture on camera, such that no verification can be made on this point.

To further investigate the lens, a ray fan was traced through the lens, see figure 31. A ray fan is a two dimensional light source with the shape of a fan, see figure 31. The angular distribution of rays can be set to cosine, which will be the equivalence of the LED intensity profile (lambertian emitter). Thus, the density of rays on the target is related to illuminance (not identical since the target is planar instead of hemispherical). In figure 31, only the upper half of the fan is ray traced since the lens can be considered to be circularly symmetric. The lens has four optical actions, see figure 31. In action 1, rays do not satisfy the TIR condition and fall well outside the camera FOV. In the spot position diagram the three rays from action 1 are visible at the expected location. Noticeably, the rays are unaffected by the curved outer surface of the lens. In action 2 and 3, the outer TIR surfaces redirects light towards the lower parts of the scene. In action 4, the continuous center surface of the lens redirects light towards the upper parts of the scene. The center of the lens (the optical axis) is marked with a red line in figure 31.

When increasing the number of rays in the ray fan and allowing both sides of the fan to be traced, see figure 32 (left), the spot position diagram in figure 32 (right) is calculated. Ray bands appear from the TIR surfaces, which can be see in figure 30, on the outer sides. In general, TIR / refraction lenses suffer from low imaging capabilities and are often associated with the issues described above. Since the lens is designed by a third party, influencing the design parameters can be difficult. Developing a workflow model for camera flash lenses including discussions with third party could increase component efficiency.

From the simulation data, the illuminance at 1 m (namely the SI-unit *candela*) can be calculated. By using a calibrated photodetector, the measured and simu-

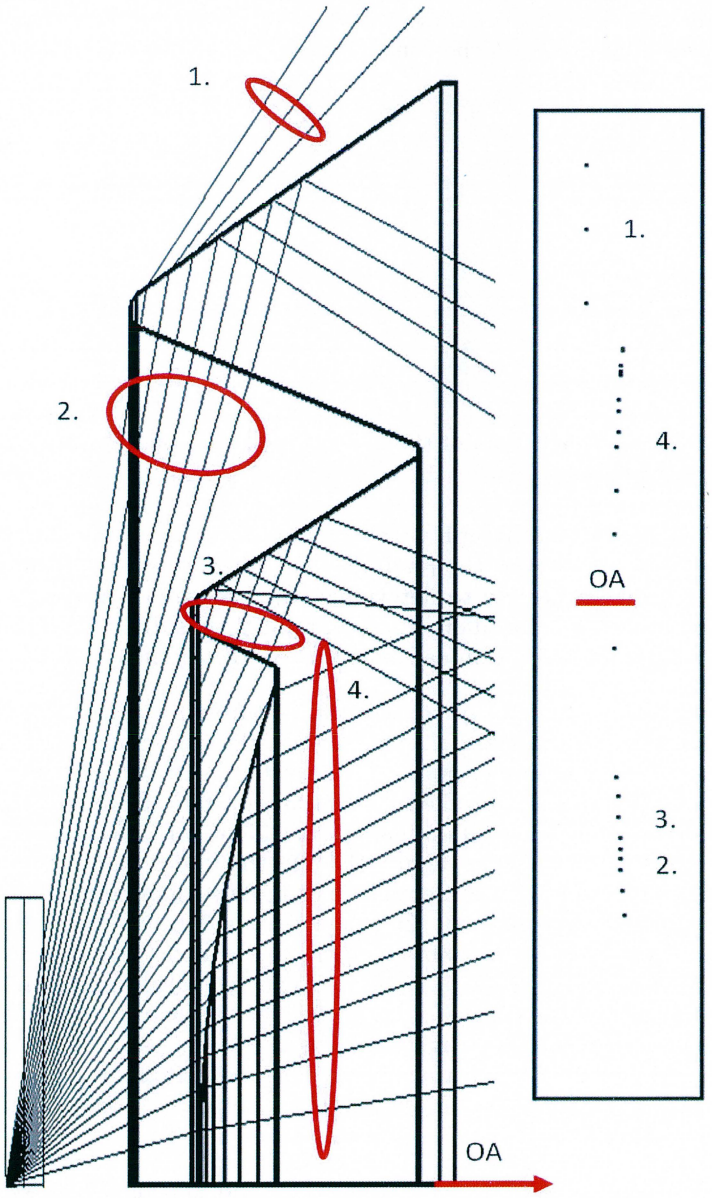

Figure 31: Ray tracing of the camera flash lens in Project 1. The optical axis (OA) is marked with a red marker in the 2D view (left) and the spot position diagram (right)

lated center illuminance can be compared. In simulations, the center illuminance value was approximately 107 lx, see figure 33. The value is averaged over a small area, comparable to the area of the photodetector. The measured value from the photodetector was 113 lx. Illuminance values at other distances are calcu-

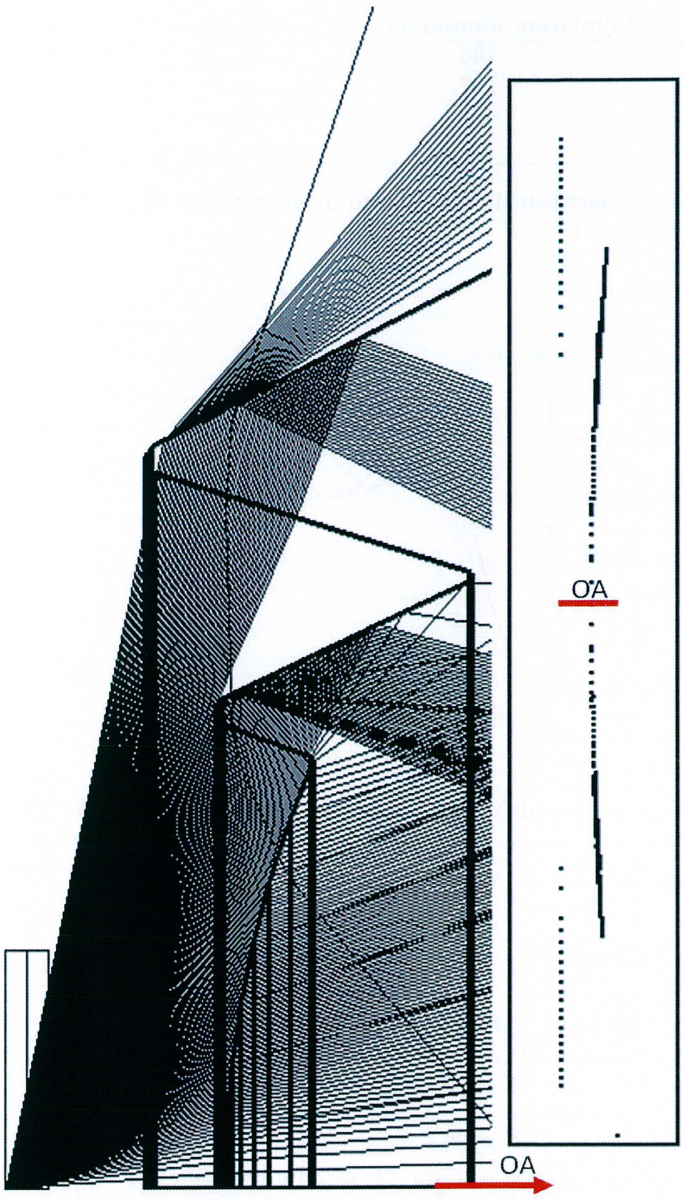

Figure 32: Ray tracing of the camera flash lens in Project 1. The optical axis (OA) is marked with a red marker in the 2D view (left) and the spot position diagram (right)

lated using r^{-2} falloff (since the focal length of the camera flash lens is small), see table 3. Measurements at 0.5 m and 2 m are extrapolated from the 1 m measurement using a r^{-2} relationship, due to measurement setup limitations.

Distance (m)	Simulation illuminance (lx)	Measured illuminance (lx)
0.5	436	452
1	107	113
1.5	50	50
2.0	28	28

Table 3: Comparison between simulated and measured center illuminance of the camera flash in Project 1

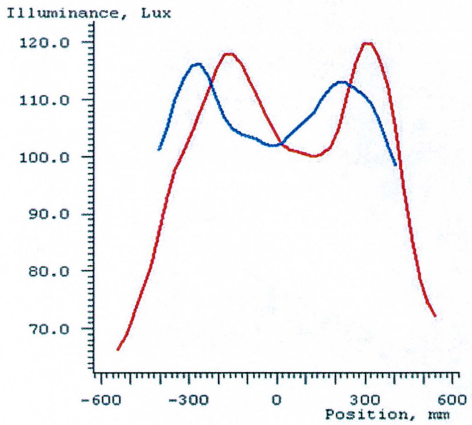

Figure 33: X slice (red) and Y slice (blue) of illumination profile at 1 m in Project 1.

3.1.2 Proximity sensor

In project 1, the proximity sensor had an issue where it all times indicated that an object was in proximity to the handset. The only explanation for this issue is optical short cut of the proximity device. Optical short cut occurs when surrounding geometry of the IR emitter scatters sufficient amounts of IR radiation to trigger the IR sensor. Examples of surrounding geometry can be the proximity sensor front window or proximity housing. The issue only appeared in white plastic models, whereas it could be concluded that the issue could be related to the white plastic which encloses the proximity device. The geometry of the proximity device can be seen in figure 34 (left). The assumed ray path for optical short circuit can be seen in figure 34 (right). By importing a STEP model of the proximity device into Solid Works, the geometry could be simplified and unnecessary details could be removed. When imported to the simulation software, optical properties could be assigned. According to the specification of the IR-emitter, the peak wavelength was centered around 940 nm, where knowledge and measureablility of optical properties of plastic is limited. The relevant property of the plastic material is the reflectance. As a first approximation, the reflectance was measured at 760 nm and the result

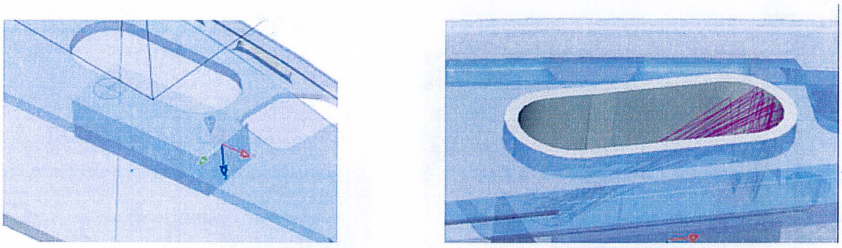

Figure 34: 3D view of the proximity sensor geometry in Project 1

extrapolated to reflectance at 940 nm. For reference, the black plastic was also measured. The proximity device itself and the proximity front window was set to 1 % reflectance with lambertian angular cross section.

A technical specification for the IR emitter stated an emittance angle of 30 degrees, which was also assigned in the model. The acceptance cone of the IR receiver was assigned in the model to 70 degrees, according to the IR receiver technical specification. In order to achieve the acceptance cone on the receiver, a filter was placed on the receiver to filter out rays with incident angle higher than 35 degrees half-angle. The measured values for the plastic colors are found in table 4

White plastic reflectance (%)	Black plastic reflectance (%)
70	0.3

Table 4: Measured reflectance values

Two simulations were performed, one with the white plastic reflectance value and one with black plastic reflectance value. The results of the simulation can be seen in figure 35 (not normalized): As expected, the white plastic resulted in higher irradiance of IR light on the receiver. The incident radiometric flux ratio between white and black plastic was 50 times higher in the simulation where white plastic was used. The following conclusions could be made:

- A black print on the white plastic inside the proximity device housing can be used to limit optical short circuit
- Additional counter-measures should be applied since the spatial tolerance of the proximity device could result in increased scattering if the proximity device approaches the housing walls

Sometime later, the first samples with the black print arrived from production, see figure 36 (right). For comparison, the original white plastic model is seen in figure 36 (left) The solution was successful and the issue was solved. As additional counter-measure, a gasket was placed inside the proximity housing. The gasket has a wall between the IR emitter and the IR receiver, however the need for the black print was not eliminated as IR light can propagate inside the proximity window. Another advantage of the gasket is the dust protection.

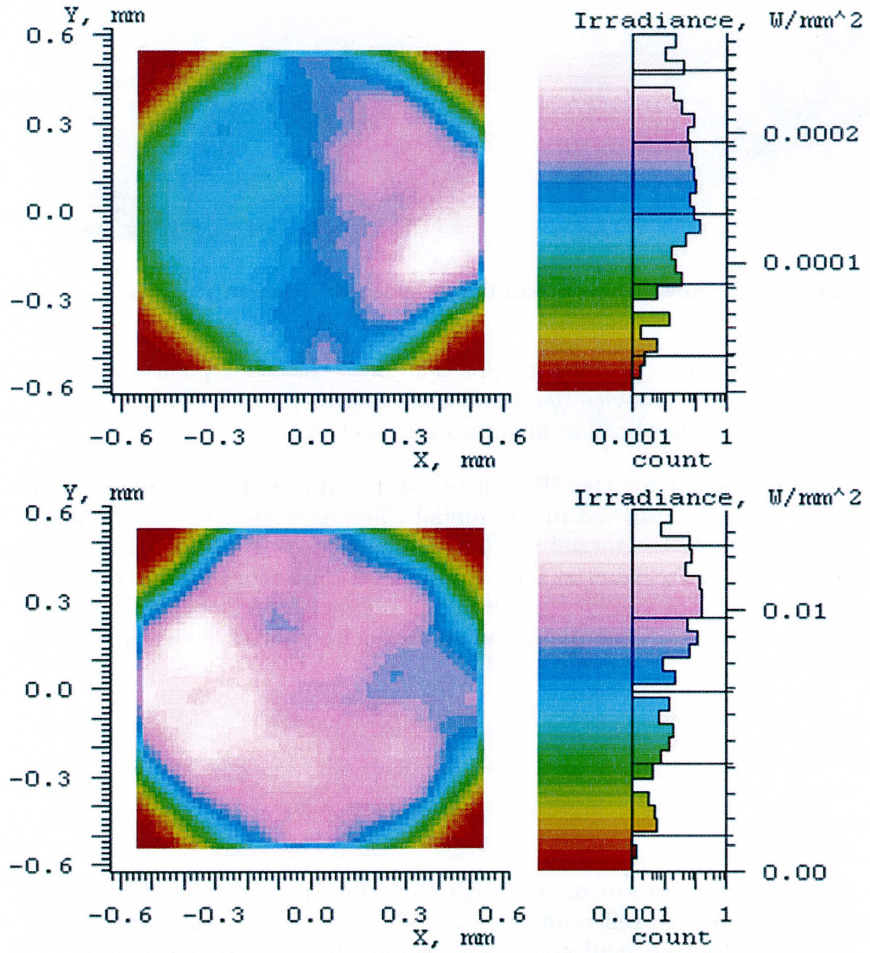

Figure 35: Simulation results of the optical circuit level for surrounding geometry in black (top) and white (bottom). Note the irradiance scale.

Figure 36: Comparison between white plastic model and black print model of the proximity geometry in Project 1

In summary, although approximations were crude, simulations effectively verified the issue, solutions could be proposed and the issue solved.

3.2 Project 2

3.2.1 Camera flash

In project 2, the implementation of the camera flash lens was challenging due to spatial constraints. Two lens designs from a third party were considered. An extensive comparison was made to find the best tradeoff between lens gain, uniformity, spatial tolerance sensitivity and spatial occupancy. The first of the two lenses was a Fresnel lens and the second was a Fresnel / TIR hybrid lens. The lens material was PMMA and the LED model could be imported from the model library in the simulation software. A detector coaxial with the camera scene at 1 meter was created. Typical spatial tolerances are 0.25 mm in the x-y plane (the circuit board plane) and 0.1 mm in the z-direction (perpendicular to the circuit board plane). Since spatial tolerances are relatively small, caution must be taken when positioning the LED with the lens. Large amounts of rays are needed since the lens to scene distance is 1 m and detector resolution must be sufficient to detect inhomogeneities.

The lens design was assigned to PMMA material and the LED was configured using the datasheet from the manufacturer. The Fresnel lens had, according to the third party, good performance, although the lens had large spatial occupancy. In the simulations performed, an 1115x836 mm^2 detector was placed 7.895 mm off LED optical axis. At 500 mA, the LED luminous flux was 135 lm. 80 millon rays were traced.

In figure 37, the LED was positioned 0.25 mm off the lens optical axis in x- and y-direction, respectively. Noticeable effects can be seen in this worst case scenario. When simulating a $\pm$ 0.1 mm displacement on the z-axis, the results

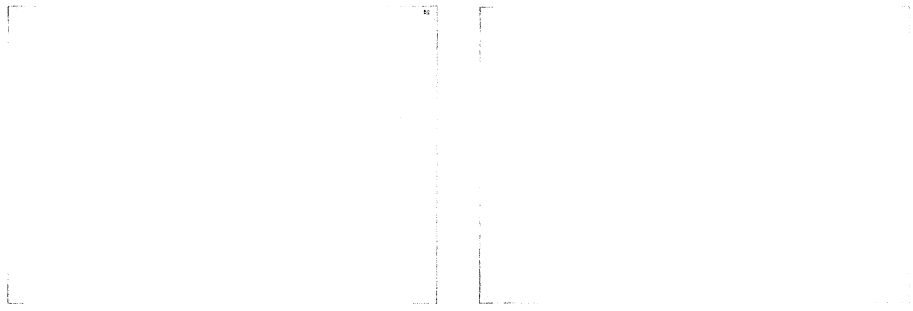

Figure 37: RGB Raster chart of the camera flash beam profile in Project 2 (Fresnel lens design). To the left, the LED is placed 0.25 mm off the lens optical axis in the x-direction. To the right, the LED is placed 0.25 mm off the lens optical axis in the y-direction.

in figure 38 are produced. The focal length of a camera flash lens is typically a few millimeters. Consequently, small alterations in z-position can yield large differences on the illuminated scene. At 0.1 mm, these differences are small, yet noticeable. Note that the illuminance in the RGB raster charts is not normalized and are for structural analysis only. For reference, the nominal position

Figure 38: RGB Raster chart of the camera flash beam profile in Project 2 (Fresnel lens design). To the left, the LED is placed +0.1 mm in the z-direction (towards the lens). To the right, the LED is placed -0.1 mm in the z-direction (away from the lens).

is seen in the figure 39. For the spatial tolerance simulations, the main aim is

Figure 39: RGB Raster chart of the camera flash beam profile in Project 2 (Fresnel lens design). The LED is placed in the nominal position

to analyze the beam deformation since lower illuminance is acceptable. In the nominal position, the illuminance on the target is the performance indicator. As previously mentioned, the luminous flux of the LED was 135 lm at 500 mA. It can be useful to find the ratio between LED and incident on target luminous flux. For the Fresnel lens in the nominal position, the luminous flux on target was 79.2 lm. Thus, a ratio of 58.6 % was calculated. As mentioned in chapter 2.1.6, the ratio can be improved close to 100 %, with an equal loss of uniformity. The center illuminance using the lens is 90 lx, see figure 40. When removing the lens, a center illuminance of 40 lx is found. The lens gain is therefore 2.25, for ideal optics (no Fresnel losses or surface structures). The second alternative, a Fresnel / TIR lens, was also investigated. The Fresnel / TIR lens was appealing due to smaller spatial occupancy. However, simulation showed that it suffered from inhomogeneities, see figure 41. The optical performance was 93 % luminous flux of the Fresnel lens. It was concluded that the Fresnel / TIR lens was unsuitable for this project. The simulation results presented above were performed in the concept phase of the project to evaluate two lens designs under consideration. At a later time, prototypes with the chosen lens arrived

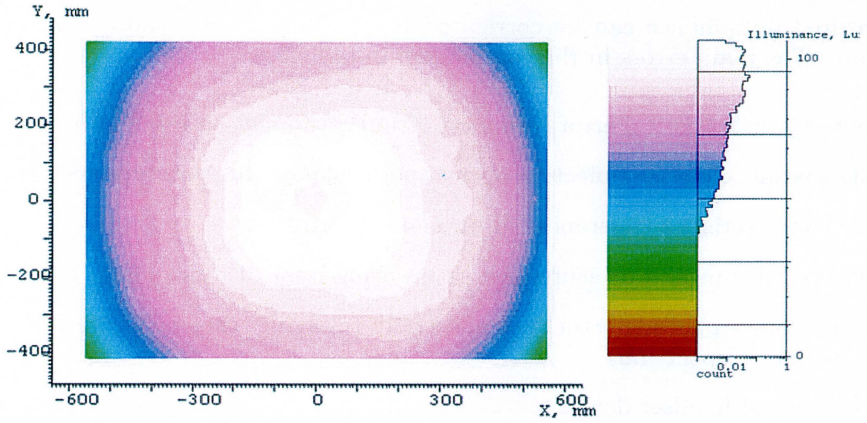

Figure 40: Illuminance Raster chart of the camera flash beam profile in Project 2 (Fresnel lens design). The LED is placed in the nominal position

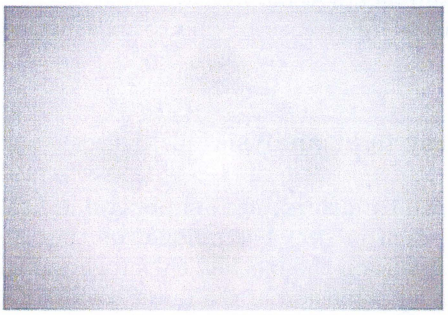

Figure 41: Illuminance Raster chart of the camera flash beam profile in Project 2 (Fresnel / TIR lens design). The LED is placed in the nominal position

for evaluation. Normally, the optical performance is measured at 1 meter. However, other distances can also be of interest. To make a correlation between real measurements and a simulation of the performance, four distances were chosen. The drive current of the LED was set to 1.5 A corresponding to a luminous flux of 286 lm. In table 5, the comparison can be seen. In the simulation, the ideal optics approximation accounts for the elevated values. Injection molded PMMA lenses can have production related imperfections, *e.g.* air bubbles [24].

Distance (m)	Simulation illuminance (lx)	Measured illuminance (lx)
0.5	900	880 (extrapolated)
1	210	220
1.5	100	91.7
2.0	50	55 (extrapolated)

Table 5: Comparison between simulated and measured center illuminance of the camera flash in Project 2

The measured illuminance can be correlated to the simulation results within error limits. The main errors in the comparison in table 5 is:

- Monte-Carlo statistical error (around 5 % in the simulation results above)
- LED spatial tolerance (affection optical performance) in prototype tested
- LED characteristics (tolerances in luminous flux)
- Measured distance in measurement setup using laser distance meter
- Calibration of photodetector (not spectrally resolving, thus calibration is dependent on spectrum)
- Alignment of handset device

The method can be used to comprehensively evaluate the camera flash performance in the nominal case. Simulations can be performed to evaluate spatial tolerance sensitivity. Measurements at 0.5 m and 2 m are extrapolated from the 1 m measurement using a r^{-2} relationship, due to measurement setup limitations.

3.2.2 Chat camera stray light analysis

The chat camera is developed by a third-party supplier and has to be verified as a single entity. In general, each project has unique solutions for the protective glass since its geometry depends on the mechanical surrounding. The protective glass for a phone camera is an extension of the outer casing of the device and is made of scratch resistant glass (pink object in figure 42). Since the protective glass may have a complex form for attaching it to the mobile device, it can induce stray light which is not specified from the chat camera supplier. For this project, the aim of the simulation was to create a situation where stray light may be induced by the protective glass. A CAD model of the entire camera, the outer casing and the protective glass was provided including technical specifications for the parts.

The CAD model of the camera is detailed including lens package, IR filter, transparent plates and sensor. Since many of these components are irrelevant to the simulation (*e.g.* IR filter) they were removed, leaving only lens package and sensor. The lens package reduces stray light by using an aperture (center disk in figure 43), thus, by including the lens package, the accuracy of the simulation result increase. However, the spatial resolution in the CAD models is not high enough for some optical surfaces (such as lens surfaces) to give an exact representation of the lens.

Two options were presented; using the lens package for model correlation or removing the lens package (imaging capabilities are lowered). The lens package is important since it is designed to eliminate stray light (by using apertures). In both cases the model correlation is lowered, however, in the first option, the model correlation loss is minimized and was therefore chosen.

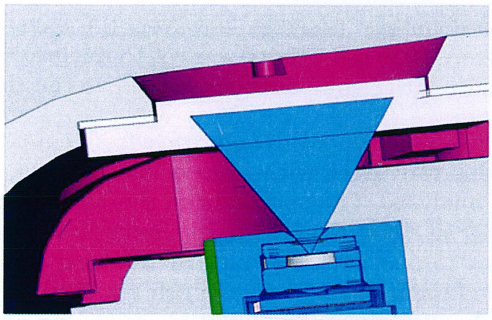

Figure 42: 3D model of the chat camera in Project 2

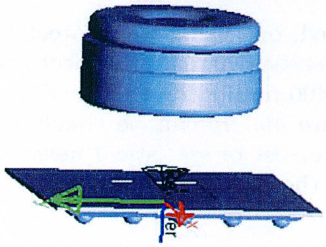

Figure 43: 3D model of the lens package of the chat camera in Project 2

The upper surfaces of the casings of the camera device were replaced with planes to increase simulation speed. Native geometry (geometry created in the simulation software) is traced with increased speed. An aperture with identical dimension to the camera casing entrance aperture was also created, see figure 44. The inner and outer casing of the mobile devices was also represented with

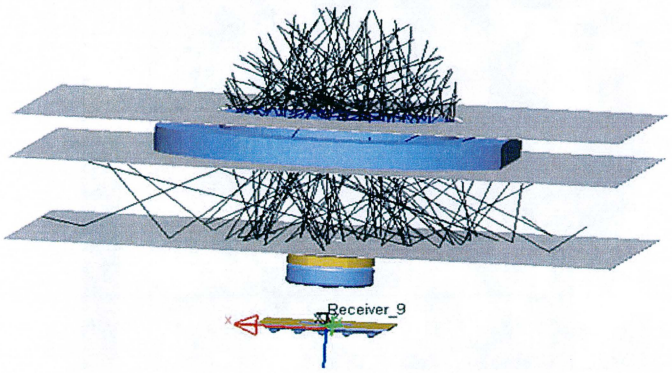

Figure 44: Simplification of the chat camera model. The simplified model was used for the optical simulations. The hemispherical light source can be seen surrounding the protective glass window (geometry of the light source is hidden)

planes. In order to allow rays to scatter inside the camera and mobile device, all surfaces were assigned lambertian scattering with 10 % reflectivity. Scattering

inside the components is definitely possible, however, the exact reflectivity is difficult to identify, therefore 10 % reflectivity was set to make sure that scattering events takes place and relative ray power stayed above the threshold value.

A hemispherical light source was created to allow rays from entering the camera from all directions. In this way, light with all possible incident angles will be tested in the stray light analysis. The spectrum of the hemisphere source was set to black body radiator at 6500 K and the luminous flux was set to 20 lm. Since the receiver was set to photometric, the rays entering the detector have to be weighed against the luminosity function, which removed IR and UV radiation from the black body spectrum. The hemisphere source was assigned an aim area. An aim area is a defined area which rays leaving the source always will aim towards. The aim area was placed on the protective glass window.

Two simulations were performed, one using the protective glass and one without the protective glass. The receiver had a 4:3 aspect ratio and utilizes 40x30 bins. Both simulations traced 400 million rays. The difference between the two simulation can be seen in figure 45. It can be concluded that the difference of the two simulation results consist of statistical noise from the Monte-Carlo nature of the simulations, *i.e.* the protective glass would not induce any stray light effects.

Two types of stray light exist. Stray light can either be spatially localized on the detector to form distinctive patterns. Alternatively, stray light can be spread over the entire detector and make the image "milky". In the case of the latter form of stray light, it would be hard to detect in the result from the simulation. Additional simulations could be performed and ray paths analyzed, however, time limitations prevented further simulations.

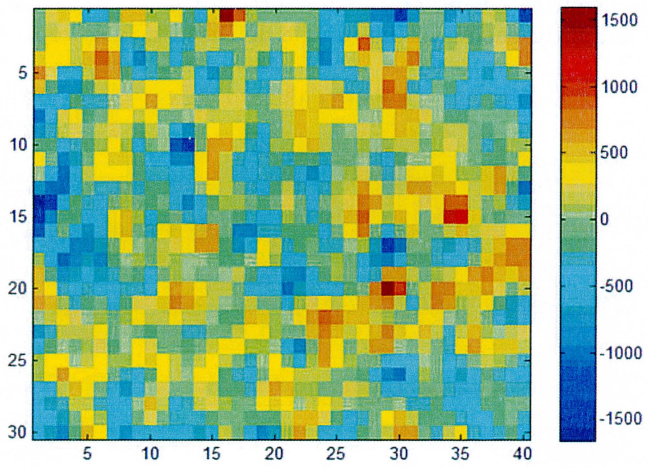

Figure 45: The computed difference between the simulation result when including the protective glass and the simulation result when excluding the protective glass

3.2.3 Main camera stray light analysis

The main camera of the project uses a chrome ring around the camera protective glass for esthetical reasons. Concerns of stray light were investigated in this simulation project. As opposed to the previous simulation of the chat camera, no camera specifics were included since CAD models were unavailable. The aim area of the hemispherical light source was placed over the entire chrome ring and the detector was placed on the protective glass, see figure 46. The chrome parts were set to mirror coating (*i.e.* 100 % reflection for all wavelengths and rays obey the law of reflection when incident to the surface). The previously

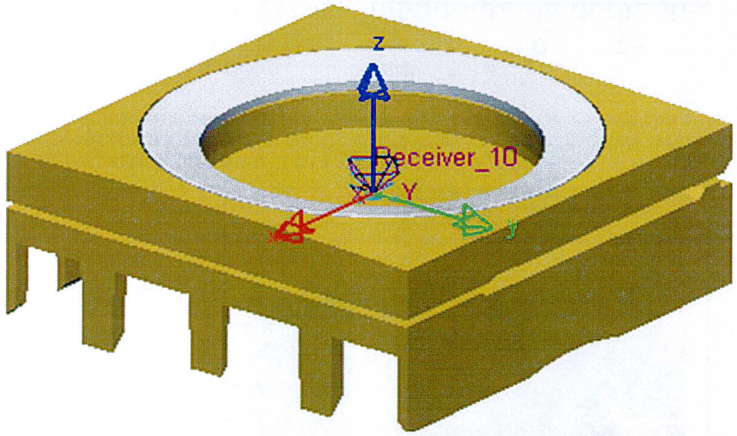

Figure 46: 3D model of the main camera chrome ring (light grey) with surrounding geometry (yellow)

described hemispherical light source (see page 57) was used to allow rays to enter the camera from all directions. The free optical path from the light source to the detector resulted in that most traced rays would not be reflected on the chrome ring. On the detector surface, the strong signal from the direct illuminance from the hemisphere could possibly drown the stray light from the ring. Consequently, a filter on the detector was applied which allowed only rays that satisfied one of two conditions to enter the detector:

1. Ray intersection with top chrome surface
2. Ray intersection with edge chrome surface

The result of the simulation can be seen in figure 47. From the results in figure 47, it is clear that the stray light resulting from reflection on the top chrome surface is negligible compared to the stray light induced by the chrome edge. From a geometrical point of view, the results are not surprising as the top chrome surface has an angled cut to minimize reflected light to enter the camera. An important observation is CAD model-to-production correlation. The chrome edge induces stray light in the simulations due to the large extent of the edge area. The size of the edge is small and when produced, the shape might be

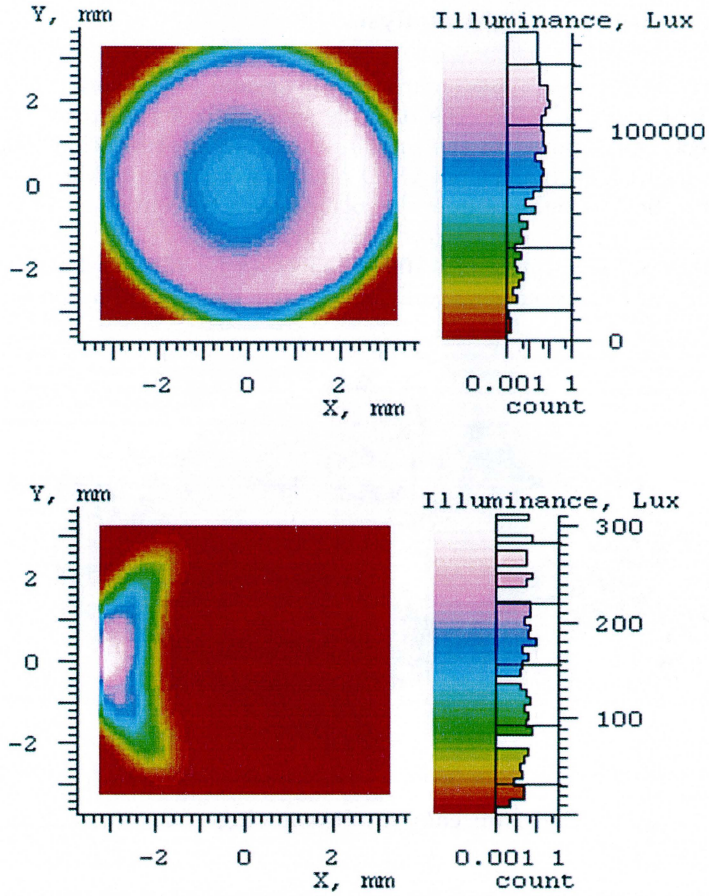

Figure 47: Illumination raster of the stray light induced by 1. top chrome surface (bottom) and 2. edge chrome surface (top)

subject to change. In figure 48, a microscope image of the cross section of the chromed ring is seen. The chrome edge can be seen to the left in figure 48. As seen in the figure above, the chrome ring has a rounded geometry, as opposed to the straight contour in the CAD model. Consequently, the stray light effect seen in the simulations would be minimized for this geometry.

The chrome ring and hemisphere light source are circularly symmetric (when the number of traced rays is high) which should result in a circular symmetric stray light profile. However, the results in figure 47, have an illuminance profile which is asymmetric. The asymmetry is due to the coordinate axes of the two parts (hemisphere and camera) are aligned. When aligned, the freeform surface of the outer shell, on the camera side becomes unaligned with the hemisphere light source.

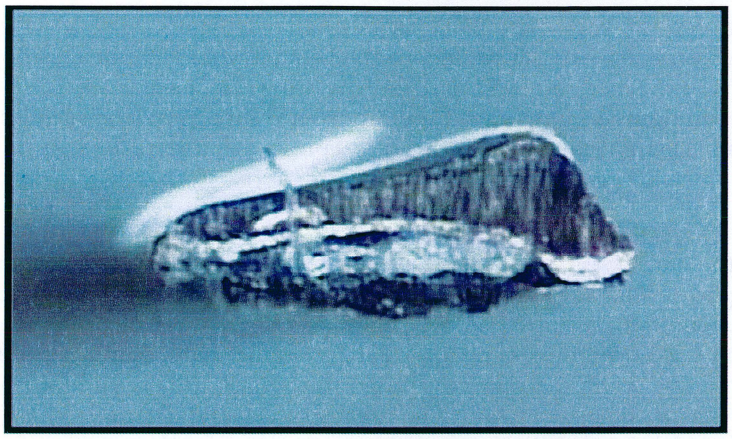

Figure 48: Photographic image displaying a cross section of the main camera chrome ring in Project 2

3.2.4 Keypad backlight

For keypad illumination, light guides are typically used to guide the light from a local LED to the key. White paint dots can be used to allow light to escape from the light guide and towards the key. Developing light guides can be costly since high precaution must be employed to ensure that light is correctly directed. If so, successful results are often obtained. In this project the LEDs where in proximity of the key and the key illumination profile was a small homogeneous area. A hard plastic key is normally attached to a flexible silicone mat. There are several reasons for using a flexible mat. The hard key is pushed to connect a metallic dome, with a built in spring load, to a circuit board. The flexible silicone mat helps in connecting the force from the key to the metallic dome. The silicone is also used as a diffuser to conceal the electronics below it. The silicone is semitransparent with high haze value. The high haze value property is used as a light guide in this project. As figure 49 presents, the silicone mat

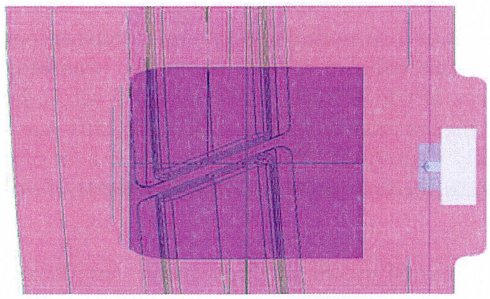

Figure 49: 3D model of a silicone mat in Project 2.

was extended towards the LED (purple segment) to increase light coupling efficiency. The aim was to scatter light inside the silicone material to illuminate

small gaps between the keys. The LED was a small side firing white LED (seen to the right in figure 49). A CAD model of the geometry was imported into the simulation software. Since the LED used in this project is a standard LED, the configured the configured model could be imported from a previous simulation, in which it had been specified according to a specification datasheet from the supplier.

The information needed for the simulation where thus optical properties for the silicone mat, the surface of the plastic covering the keys and for the surface of the key themselves. The keys are chromed plastic and were set to mirror properties .The silicone mat is harder to specify since the process involves volume scattering events. As described in chapter 2.4.1, volume scattering is a complex physical process and is hard to specify in greater detail. There are two main techniques to deal with the problem. The first is measuring a sample of the silicone mat and match to some volume scattering model, *e.g.* Henvey-Greenstein scattering model. The experimental setup for this type of measurements is quite complex. Consequently, samples have to be sent away to third party for analysis.

Alternatively in the second technique, a general volume scattering model can be used which scatters light uniformly in all directions. The advantage of the second technique is the simplicity of the model. A measurement is carried out to find the transmission of the sample, if the sample is semitransparent. In this way, the object becomes semitransparent with a volume scattering effect superimposed.

Using the second technique, simulations were performed on the keys. To clearly see the spatial profile of the light, photorealistic renderings were generated. The rendering can be seen in figure 50. The color of the LEDs in the rendering does not correlate to the photograph color since the computer monitor, optical simulation software and the camera were not calibrated to the same color space. Extensive calibration work must be performed to ensure that all of the components mentioned above have the same color space and therefore calibration was neglected. To reduce the possibility of misleading results created from uncalibrated color spaces, the result is presented in grayscale.

Volume scattering simulations are usually very time-consuming. For comparison, a fast alternative to the volume scattering model was simulated. In the fast alternative, all surfaces of the silicone material were set to lambertian scattering property and volume scattering was disabled. In this way the number of calculations was drastically decreased. The photometric flux of the rays has to be decreased to compensate for the additional path length of volume scattered rays.

When comparing the illuminance profile of the volume scattering results and the illuminance profile of the surface scattering results with the illuminance profile of the photographic image (figure 51) a correlation can be identified. Although, more precise optical properties of the silicone mat is needed to successfully compare the simulated result with the camera photograph. It should be noted that the an accurate comparison can be tedious since all of the measurement equip-

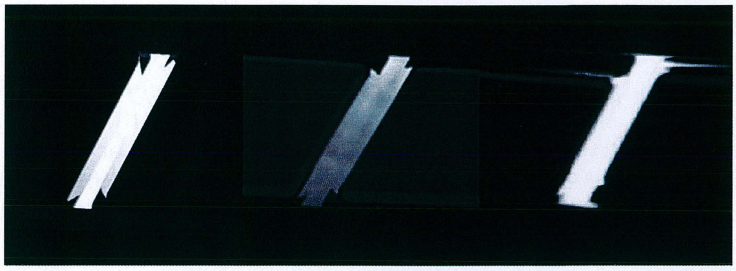

Figure 50: Left: Photorealistic rendering of the illumination profile using volume scattering properties. Center: Photorealistic rendering of the illumination profile using surface scattering properties. Right: photographic image of the illumination profile (prototype build)

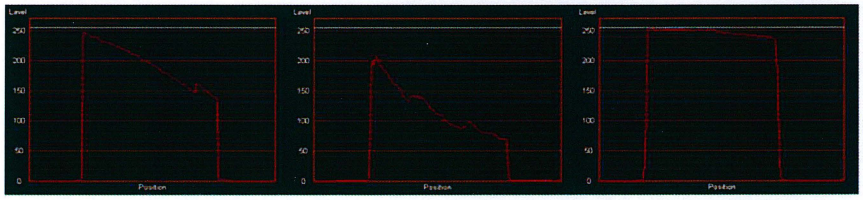

Figure 51: Illuminance profile of the images in figure 50 (from top to bottom), respectively.

ment (monitor for simulation and camera for photograph) is not calibrated. The result is adequate to suggest that guiding the light using the silicone support mat of the keys will be successful. In received prototype builds using the silicone mat as a light guide the illumination effect was approved.

3.3 Project 3

As previously discussed, some simulation cases are limited to comparative values or qualitative simulation results. In this simulation project, the goal was a more advanced comparative study. A released product was used as a reference project. The feature under study was the proximity sensor and the ambient light sensor, which used the same components in both projects. Thus, efforts could be invested into making the surrounding mechanics the differentiating factor. Since the functionality of the proximity sensor and ambient light sensor in the reference project was successful, it could be used as a performance indicator.

3.3.1 Proximity sensor

The proximity sensor simulation had two goals:

- Measuring the optical short circuit level
- Measuring the signal level when an object is in proximity (ideally, a skin type object)

Both simulations were performed in both projects. As previously described (in Project 1), the plastic cover color has significant importance when analyzing optical short circuit in proximity devices. For this reason, a worst case scenario of white plastic (70 % lambertian scattering) was set to the plastic cover. A technical specification was used to specify the IR detector and IR emitter. One interesting aspect of the IR detector is the spectral response. The spectral response of the IR detector can be compared to the luminosity function of the eye, except that the spectral response of the IR detector peaks at 940 nm, where the IR emitter has it peak emission wavelength. In the optical simulation software, a spectral response function was not added. Since both projects uses the same detector it would suffer the same losses when including the spectral response function. No scattering mechanisms in the models are wavelength specific such that it can *e.g.* prefer a specific wavelength in one of the models.

Volume scattering property was set to the black gasket surrounding the proximity device (mean free path = 0.06 mm and uniform angular scattering cross section). No reflectance was added to the gasket surface since the small percent of scattering (around 0.3 %) would not affect optical short circuit. The CAD model also included a thin layer of adhesive for mounting the proximity window. The used adhesive is optically transparent in the visible spectrum, however, it has a slight diffusive effect. Adhesive is necessarily not matched (in terms of refractive index) to the polycarbonate proximity window. It can be concluded however, that the index of refraction of the adhesive and the polycarbonate are reasonably comparable to approximate the adhesive as an extension of the proximity window. In figure 52, a 3D model of the proximity sensor in the reference project is seen. The gasket thickness is thick enough to eliminate most rays that undergo volume scattering events. Most of the rays entering the IR receiver are scattered inside the proximity window.

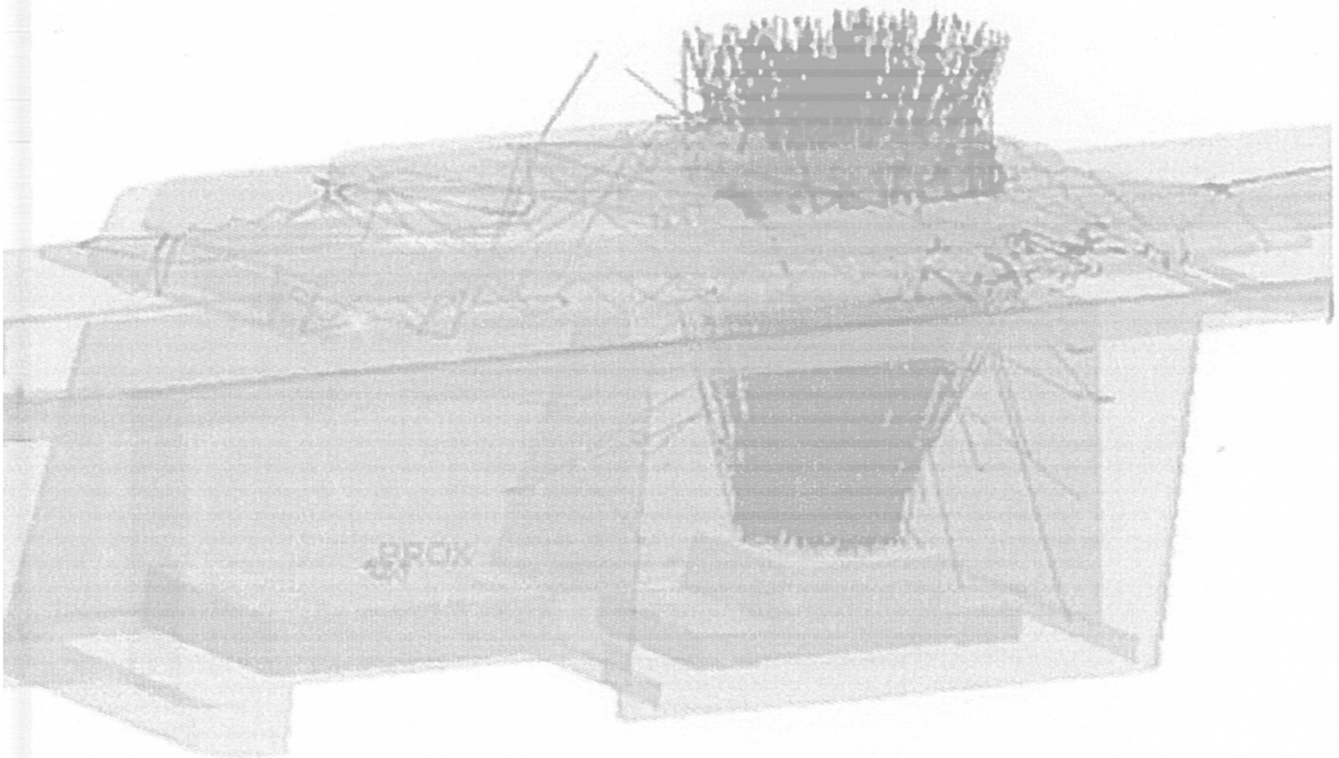
BROIX

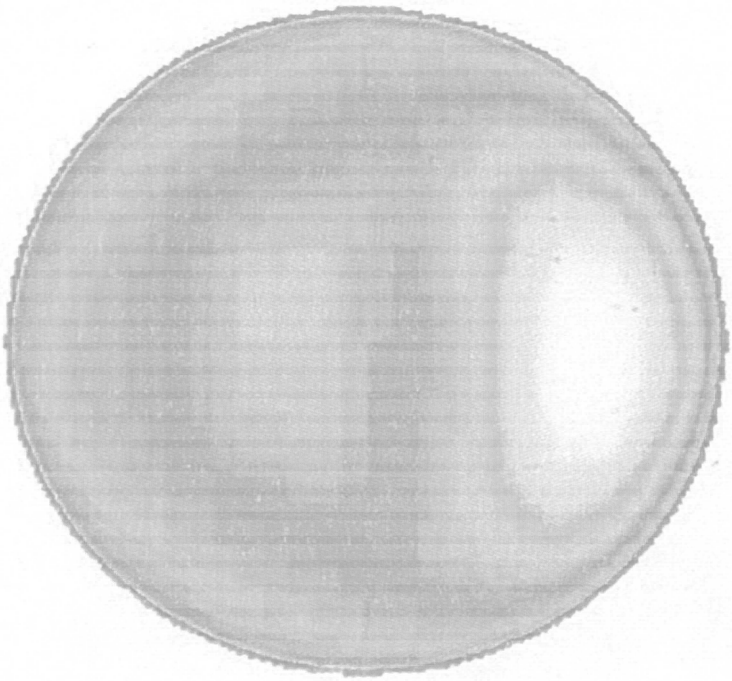

esthetic value from a design point of view. In figure 57, the first design of the ALS window has been ray traced using the same hemispherical light source as described on page 57. For esthetical reasons, the upper side was shaped after the geometry of the handset. The upper side has a lens effect and directs most rays to start reflecting inside the window. The added bottom cylinder prevented rays from reaching the ALS. An identical setup in the reference project was also

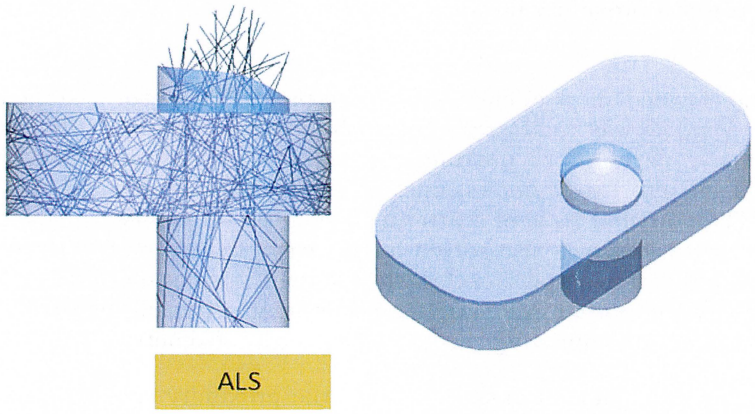

Figure 57: 3D model of the ALS window in Project 3

simulated. Two simulation cases where performed:

- Hemispherical light source
- Highly directional, collimated light source for detecting angular performance

The hemispherical light source had a total of 1700 lm luminous flux. In the reference project 6.11 lm reach the ALS. This could be compared with a total of 0.018 lm for Project 3 (*i.e.* ratio of 0.18 %).

When tracing rays from the highly directional light source, rays with high incident angle from the left side in figure 57, were unable to reach the ALS due to the lens effect in the window.

In the new design, the upper side of the window was reconstructed to avoid the lens effect. The bottom cone was eliminated and a diffusive structure was applied to the lower side of the ALS window. With the implementations, the luminous flux on the ALS was 6.56 lm, *i.e.* slightly better than the reference project. No mentionable issues were detected using the directional light source.

3.4 Project 4

indicator

3.4.1 LED Status

ow for status
ojection of a LED beam on a diffusive wind
PET) thermo-
ow is made of Polyethylene terephthalate (P
d one red) are
usive layer (10 m). Two LEDs (one white an
illuminating
usive window on a PCB, see figure 58. By
, messages can be mediated to the end user
e.g. loading
lluminate the
are lambertian emitters, and if allowed to i
Project 4 uses the pr
indication. The wind
plastic and a thin diff
placed behind the di
the window, differen
status. Both LEDs

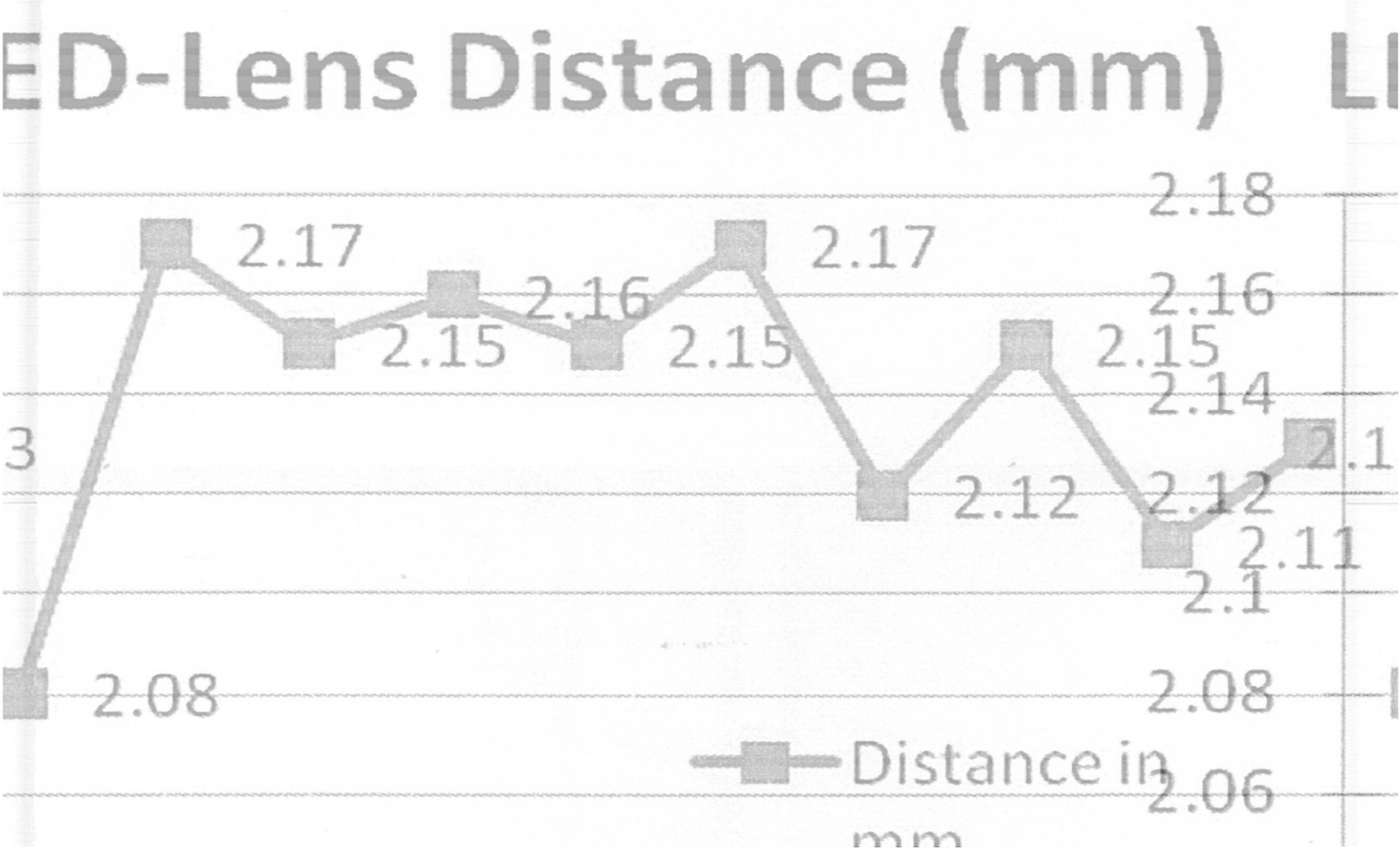
ED-Lens Distance (mm) LI
2.18
2.16
2.14
2.1
2.08
2.06
2.17
2.15
2.16
2.15
2.17
2.12
2.15
2.12
2.11
2.1
2.08
Distance in mm

3.6 Project 6

3.6.1 QWERTY keyboard